University of Alberta

Effects of combined creatine and hypothermia following neonatal hypoxic-ischemia

by

Scott Leighton Hess

A thesis submitted to the Faculty of Graduate Studies and Research
in partial fulfillment of the requirements for the degree of Master of Science

in

Neurochemistry

Department of Psychiatry

Edmonton, Alberta
Spring, 2008

Library and Archives Canada

Published Heritage Branch

395 Wellington Street
Ottawa ON K1A 0N4
Canada

Bibliothèque et Archives Canada

Direction du Patrimoine de l'édition

395, rue Wellington
Ottawa ON K1A 0N4
Canada

Your file Votre référence
ISBN: 978-0-494-45820-4
Our file Notre référence
ISBN: 978-0-494-45820-4

NOTICE:
The author has granted a non-exclusive license allowing Library and Archives Canada to reproduce, publish, archive, preserve, conserve, communicate to the public by telecommunication or on the Internet, loan, distribute and sell theses worldwide, for commercial or non-commercial purposes, in microform, paper, electronic and/or any other formats.

The author retains copyright ownership and moral rights in this thesis. Neither the thesis nor substantial extracts from it may be printed or otherwise reproduced without the author's permission.

AVIS:
L'auteur a accordé une licence non exclusive permettant à la Bibliothèque et Archives Canada de reproduire, publier, archiver, sauvegarder, conserver, transmettre au public par télécommunication ou par l'Internet, prêter, distribuer et vendre des thèses partout dans le monde, à des fins commerciales ou autres, sur support microforme, papier, électronique et/ou autres formats.

L'auteur conserve la propriété du droit d'auteur et des droits moraux qui protège cette thèse. Ni la thèse ni des extraits substantiels de celle-ci ne doivent être imprimés ou autrement reproduits sans son autorisation.

In compliance with the Canadian Privacy Act some supporting forms may have been removed from this thesis.

While these forms may be included in the document page count, their removal does not represent any loss of content from the thesis.

Conformément à la loi canadienne sur la protection de la vie privée, quelques formulaires secondaires ont été enlevés de cette thèse.

Bien que ces formulaires aient inclus dans la pagination, il n'y aura aucun contenu manquant.

Canada

ABSTRACT

Neonatal hypoxic-ischemia (HI) is a frequent cause of brain damage contributing to many disorders. One of the most effective treatments for HI is hypothermia, although its effectiveness is limited. To improve hypothermia's effectiveness, combination treatments that enhance hypothermia's mechanisms of action need to be investigated. Both creatine (Cr) and hypothermia are theorized to derive their neuroprotective benefits from energy recovery. To investigate the combination of Cr and hypothermia, a post-natal day 7 rat pup model of HI was utilized. After HI, animals were treated with 24 hours of hypothermia and Cr/glucose infusion. Cr was injected for 4 consecutive days after hypothermia and damage ranking, infarct volume, white matter thickness, cytochrome c expression, and TUNEL staining were examined. Results showed Cr to have non-significant neuroprotective effects alone and in combination on all measurements except white matter thickness. These results may indicate that increased neuroprotection may not be possible through energy recovery.

ACKNOWLEDGEMENT

Firstly, I would like to thank my supervisor Dr. Kathryn Todd for all her patience and understanding over the last two years. I would also like to sincerely thank my co-supervisor, Dr. Jerome Yager who has provided me with an enormous source of thoughtful input, personal direction, and intrinsic motivation over the last two years. I would also like to thank Dr. Glen Baker for giving me many second chances in the Department of Psychiatry and in the Neurochemical Research Unit as well as for serving on my graduate committee.

Many thanks also to Edward Armstrong for his technical expertise and advice, without which my graduate work would not have been possible. I also wish to express gratitude to my fellow students including Glenn Armitage (for providing me with a good conversation when I least expected it), Amy Black (for her great enthusiasm and encouragement), Kam Dhami (for helping me return safely to our office after our trips to Marco's), Lauren Jantzie (for great technical assistance), Melissa Kelly (for still more technical assistance), Aaron Lai (for helping me mop up some ugly messes over the last two years), and Shawna Pandya (for showing me how to apply trimethylxanthine to research).

I would also like to thank Tara Checknita for the tremendous amount of administrative assistance she has provided me including helping me to figure out when nearly everything was happening. Thanks also to Jordyce van Muyden for managing my finances and helping me solve problems while I conducted research.

TABLE OF CONTENTS

CHAPTER 1: INTRODUCTION.....1

1.1. Hypoxic-ischemic brain damage.....1

1.2. Cell death.....2

1.2.1. Mechanisms of brain cell death.....2

1.2.2. Necrotic cell death.....2

1.2.3. Apoptotic cell death.....8

1.3. Secondary energy failure following hypoxic-ischemia.....11

1.4. Post-hypoxic-ischemic hypothermia.....13

1.4.1. Hypothermia as a neuroprotective treatment.....13

1.4.2. Neuroprotective mechanisms of hypothermia.....16

1.5. Enhancing the neuroprotective effects of hypothermia.....18

1.6. Creatine as a hypothermia co-treatment.....19

1.6.1. Creatine synthesis and metabolism.....19

1.6.2. Neuroprotective effects of creatine.....20

1.6.3. Creatine and mitochondrial function.....22

1.6.4. Creatine and reactive oxygen species.....24

1.7. In vivo animal models of neonatal hypoxic-ischemic brain damage.....24

1.8. Hypothesis.....26

CHAPTER 2: MATERIALS AND METHODS.....27

2.1. Experimental animals.....27

2.2. Induction of hypoxic-ischemia.....29

2.3. Low-dose injection protocol.....29

2.4. Preliminary studies 30
2.5. Ranking of damage 32
2.6. Animal sacrifice 34
2.7. Tissue sectioning 34
2.8. Hematoxylin and eosin staining 34
2.9. Analysis of infarct volume 35
2.10. White matter analysis 35
2.11. Cytochrome c immunohistochemistry 37
2.12. Immunohistochemistry analysis of cytochrome c 38
2.13. TUNEL staining 38
2.14. TUNEL analysis 39
CHAPTER 3: RESULTS 44
3.1. General observations 44
3.2. Preliminary core temperature and blood glucose measurements 44
3.2.1. Core temperature 44
3.2.2. Blood glucose levels 46
3.2.3. Damage ranking 46
3.3. Infarct volume 46
3.4. White matter damage 50
3.5. Cytochrome c cell counts 50
3.6. TUNEL staining 50
CHAPTER 4: DISCUSSION 56
4.1. Overview 56

4.2. Neuroprotection in white matter.....56
4.3. Cytochrome c release and apoptosis.....57
4.4. TUNEL and apoptosis.....58
4.5. Creatine as a neuroprotective treatment.....60
4.6. Future studies.....62
4.6.1. Use of creatine in adults.....62
4.6.2. Creatine supplementation to unborn fetuses.....62
4.6.3. Alternative combination mechanisms.....63
4.7. Conclusions.....64
REFERENCES.....65

LIST OF FIGURES

Figure 1-1. Pathological mechanisms of cell death.....3

Figure 1-2. Signalling pathways in extrinsic apoptosis.....9

Figure 1-3. Signalling pathways in intrinsic apoptosis.....12

Figure 1-4. Time-dependent changes in ATP and PCr in PND 7 rats following HI.....14

Figure 1-5. Endogenous synthesis of Cr.....23

Figure 2-1. Lesion severity in PND 14 rats.....33

Figure 2-2. External capsule thickness.....36

Figure 2-3. Cell count fields for cyt c immunohistochemistry analysis.....41

Figure 2-4. Regions selected for TUNEL analysis.....42

Figure 2-5. TUNEL field coverage.....43

Figure 3-1. High-dose 24-hour core temperature measurements.....45

Figure 3-2. High-dose blood glucose measurements.....45

Figure 3-3. Low-dose damage ranking.....47

Figure 3-4. High-dose damage ranking.....47

Figure 3-5. Low-dose infarct volume.....48

Figure 3-6. High-dose infarct volume.....48

Figure 3-7. Infarct volume representative photomicrographs.....49

Figure 3-8. H and E staining for white matter thickness analysis.....49

Figure 3-9. Analysis of anterior external capsule.....52

Figure 3-10. Analysis of posterior external capsule.....52

Figure 3-11. Cyt c immunohistochemistry photomicrographs.....53

Figure 3-12. Cyt c immunohistochemistry cell counts.....54

Figure 3-13. TUNEL expressing brain regions 54

Figure 3-14. Percentage of TUNEL coverage in lateral dorsal thalamus (A) and somatosensory cortex (B) fields 55

LIST OF TABLES

Table 2-1. Treatment groups used in the low-dose 3 mg/kg study.....28

Table 2-2. Treatment groups used in the high-dose 3 g/kg study.....28

LIST OF ABBREVIATIONS

ABC	Avidin-biotin complex
AD	Anoxic depolarization
ADP	Adenosine diphosphate
AGAT	L-Arginine:glycine amidinotransferase
AMP	Adenosine monophosphate
AMPA	α-Amino-3-hydroxy-5-methyl-4-isoxazolepropionic acid
ANOVA	Analysis of variance
APAF-1	Apoptotic protease activating factor-1
ATP	Adenosine triphosphate
Bid	Bcl interacting domain
BBB	Blood-brain barrier
CAD	Caspase-activated DNase
CC3	Cleaved caspase-3
CC6	Cleaved caspase-6
CH	Creatine hypothermic group
CK	Creatine kinase
CN	Creatine normothermic group
CNS	Central nervous system
Cr	Creatine
Cyt C	Cytochrome c
DAB	3',3' Diaminobenzedine tetrahydrochloride
DNA	Deoxyribonucleic acid

FAM	Formaldehyde, acetic acid, methanol
FasL	Fas Ligand
GAA	Guanidinoacetic acid
GAMT	N-Guanidinoacetate methyltransferase
H and E	Hematoxylin and eosin
HI	Hypoxic-ischemia
HIC	Hypoxic-ischemic control
MiCK	Mitochondrial creatine kianase
mRNA	Messenger ribonucleic acid
MRS	Magnetic resonance spectroscopy
MTP	Mitochondrial transition pore
NHS	Normal horse serum
NIH	National Institutes of Health
NMDA	N-methyl-D-aspartate
nNOS	Neuronal nitric oxide synthase
NO	Nitric oxide
NOS	Nitric oxide synthase
O_2^-	Superoxide
OH^-	Hydroxyl
$ONOO^-$	Peroxynitrite
OPCs	Oligodendrocyte precursors
PBS	Phosphate-buffered saline
PCr	Phosphocreatine

Pi	Free phosphate group
PND	Post-natal day
POD	Sheep antibody binding peroxidase
ROS	Reactive oxygen species
S	Sham group
SEF	Secondary energy failure
TBS	Tris-buffered saline
TNF-α	Tumor necrosis factor alpha
TUNEL	Terminal-dUTP-nick-end-labelling
VH	Vehicle hypothermic group
VN	Vehicle normothermic group

CHAPTER 1: INTRODUCTION

1.1. Hypoxic-ischemic brain damage

Neonatal hypoxic-ischemia (HI) brain damage is the most common cause of mortality and morbidity in the neonate (Clarkson, Sutherland, and Appleton, 2005). It occurs in approximately 2-4 per 1000 full-term births and in approximately 6 out of every 10 premature births (Vannucci and Hagberg, 2004). Up to 25% of neonates who survive an HI insult will be left with brain damage resulting in handicaps that greatly reduce quality of life.

HI is implicated as a contributing factor in several different neuropsychiatric disorders. Some disorders that have been correlated with mild HI include attention deficit hyperactivity disorder (Toft, 1999), schizophrenia (Tejkalova et al., 2006), and autism (Toga, Thompson, and Sowell, 2006). In addition to neuropsychiatric disorders, disorders including mental retardation and cerebral palsy may result when HI damage is severe (Vannucci and Hagberg, 2004).

HI brain damage is caused by many pathological events that culminate in reduction of uterine and/or umbilical circulation around the time of birth (Calvert and Zhang, 2005). Examples of events occurring at or around the time of birth that contribute to HI include premature contraction of the uterus, compression of the umbilical cord, abruptio placentae, abnormal weight gain during pregnancy, and respiratory distress syndrome (Arpino et al., 2005). HI then leads to pathological changes in cellular function, causing brain cell death.

1.2. Cell death

1.2.1. Mechanisms of brain cell death

At the cellular level, an HI insult leads to a pathological reduction in energy metabolism in brain cells resulting from reduced oxygen and blood flow. When the reduction of oxygen and blood flow is prolonged, adenosine triphosphate (ATP) and phosphocreatine (PCr) drop to critically low levels and homeostatic processes fail shortly afterwards (Calvert and Zhang, 2005). Loss of homeostatic processes leads to many pathological events, culminating in cell death (Figure 1-1). These pathological processes include cell membrane depolarization, excitotoxic glutamate release, cell swelling, activation of proteases, pathological increases in intracellular Ca^{2+}, and the production of reactive oxygen species (ROS: Calvert and Zhang, 2005).

The specific mechanisms of cell death depend on the conditions and severity of the HI insult. When energy failure is severe, homeostatic mechanisms fail rapidly, leading to organelle damage and necrotic cell death. Necrosis results in complete loss of membrane integrity and the leakage of cytoplasmic contents into the extracellular matrix (Jensen et al., 2003). Pathological changes caused by HI also lead to programmed DNA-dependent cell death (apoptosis) that occurs following a delay and involves the action of genetically regulated mechanisms (Calvert and Zhang, 2005).

1.2.2. Necrotic cell death

Areas of the brain where the largest populations of cells die due to necrotic death include areas with high metabolic rates and areas that have the greatest neuronal activity and lowest blood flow at the time of the insult (Calvert and Zhang, 2005). Some prominent areas of cell loss in the neonatal brain include the cortex,

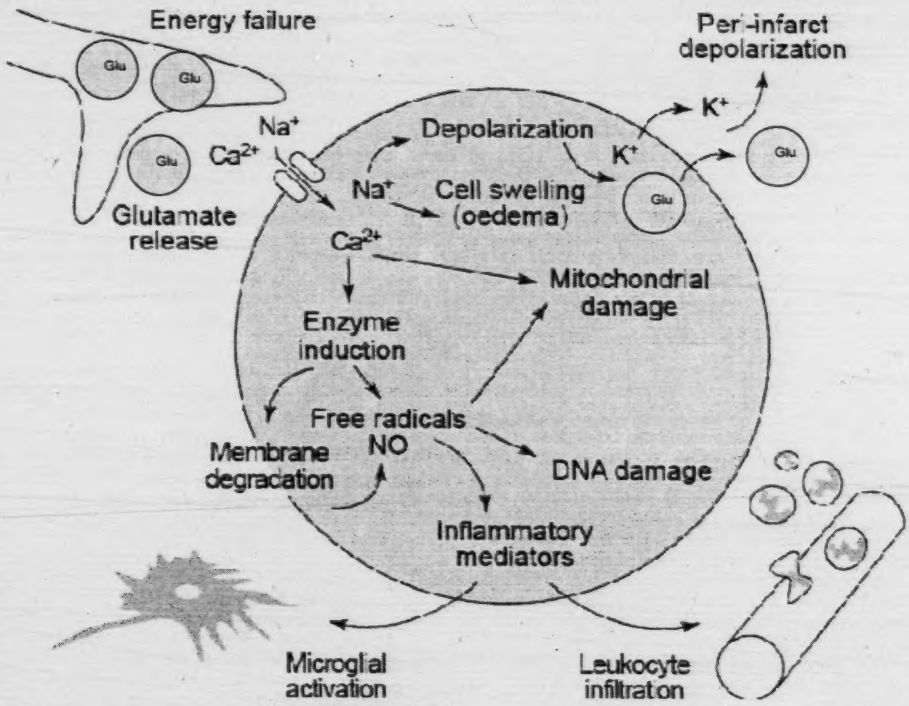

Figure 1-1. Pathological mechanisms of cell death.

Energy failure due to HI causes excitotoxic glutamate release following anoxic depolarization. Glutamate activity leads to Ca^{2+} and Na^{+} influx through ionotropic glutamate receptors. Depolarization of the cell is also accomplished by K^{+} efflux resulting in anoxic depolarization and excitotoxic glutamate release. Edema, enzyme activation, and free radical generation occur during necrosis followed by activation of inflammatory process. Once released, inflammatory mediators activate microglia and promote leukocyte infiltration of damaged tissue. Adapted from Dirnagl, Iadecola, and Moskowitz (1999).

hippocampus, and striatum. The notable morphological features of necrosis include loss of membrane integrity, release of excitotoxic quantities of glutamate, disruption of cytoplasmic organelles, and the break-down of the cell by means of lysis leading to the activation of inflammatory processes (Perlman, 2006).

Necrosis occurs when HI causes energy failure due to a complete loss of ATP and PCr (Calvert and Zhang, 2005). Energy failure leads to anoxic depolarization (AD) which is depolarization of the cell membrane caused by a lack of ATP to power ion exchange ATPases (Balestrino et al., 2002). Energy failure causes membrane ATPases to become inoperative, allowing the rapid influx of Ca^{2+}, Na^{+}, and Cl^{-} into the cell and an efflux of K^{+} from the cell. In particular, the influx of Ca^{2+} is especially harmful as it contributes to a variety of pathological physiological changes including glutamate release (Calvert and Zhang, 2005).

Once glutamate is released as a result of cell membrane depolarization, released glutamate causes Ca^{2+} influx in post-synaptic cells through the activation of glutamate receptors, primarily the N-methyl-D-aspartate (NMDA) and alpha-amino-3-hydroxy-5-methyl-4-isoxazolepropionic acid (AMPA) glutamatergic receptors (Badr Zahr and Purdy, 2006). As Ca^{2+} build-up begins after uncontrolled glutamate release, Ca^{2+} influx cannot be reversed as reuptake of glutamate cannot be accomplished by glutamate transporters due to the absence of ATP (Camacho and Massieu, 2006). The result is a chain-reaction of ion influx and continued glutamate release that damages brain cells through receptor over-activation (Calvert and Zhang, 2005). Glia are also affected by low-ATP conditions. For example, astrocytes die from ion imbalances caused by Na^{+} influx following reduced Na^{+}/K^{+} ATPase activity resulting from the

high energy requirements necessary to remove glutamate from NMDA receptors (Hazell, 2007). In white matter tracts, oligodendrocytes may be lost due to AMPA receptor-mediated glutamate excitotoxicity (McDonald et al., 1998).

In addition to excitotoxicity, the influx of Ca^{2+} also contributes to necrotic death by causing edema. Edema occurs when Ca^{2+} influx leads to altered osmotic balance that allows the entry of extracellular water (Calvert and Zhang, 2005). The build-up of high Ca^{2+} levels due to energy failure also causes the formation of damaging ROS and activates cysteine proteases in the cytoplasm beginning with calpains (Vexler and Ferriero, 2001). Once activated, calpains permeablize lysosomal membranes and cause the release of another class of cysteine proteases known as cathepsins (Golstein and Kroemer, 2007).

Cathepsins are normally used to break down proteins that are digested in lysosomes found throughout the cytoplasm. However, once cathepsins are released from lysosomes they disassemble cellular structures including proteins that comprise the cytoskeleton (actin), causing a loss of cellular membrane structure (Northington, Graham, and Martin, 2005). Other enzymes that are activated by high cytosolic Ca^{2+} levels include endonucleases responsible for the break-down of DNA, as well as lipases that disassemble lipid molecules that comprise the cell membrane (Jensen et al., 2003).

In addition to the activity of cysteine proteases, the production of ROS following energy failure also exacerbates HI damage to the brain. Once ROS levels exceed the capacity of innate scavenger molecules, excess ROS are free to damage macromolecules including DNA and ion ATPases (Moro et al., 2005). Two ROS

sources that are activated by HI include dysfunction of mitochondrial and altered nitric oxide synthase activity (Moro et al., 2005; Calvert and Zhang, 2005). Mitochondrial ROS production occurs due to the change to anaerobic metabolism by cells when substrate flow is restricted during HI (Blomgren et al., 2003).

Due to the absence of available molecular oxygen during HI, mitochondria produce ROS including superoxide anions (O_2^-) as a result of the malfunction of proteins that manage ATP-producing reactions in the electron transport chain (Zhao and Xu, 2004). One site where these reactions occur is in mitochondrial cytochrome c (cyt c), an electron transport chain protein responsible for ROS formation (Ide et al., 1999). Once cyt c no longer has an oxygen-rich environment in which it can function, it produces O_2^- which would normally be oxidized or catalyzed by adjacent proteins in the electron transport chain (Zhao and Xu, 2004). Once excess O_2^- is released from the mitochondria into the cytosol, it reacts with several molecules, forming a series of harmful ROS including peroxynitrite ($ONOO^-$) and hydroxyl (OH^-) radicals (Li and Shah, 2003).

In addition to ROS produced by mitochondrial failure, neuronal nitric oxide synthase is stimulated by the increase in Ca^{2+} and nitric oxide (NO) levels are greatly increased in response to Ca^{2+} influx (Calvert and Zhang, 2005). NO is responsible for nitration and nitrosylation of various membrane proteins and receptors including various ATPases contributing to membrane depolarization, leading to changes in membrane polarization across the mitochondrial membrane (Delivoria-Papadopoulos and Mishra, 2000). Pathologically high levels of NO damage brain cells when NO is

able to react with O_2^- forming $ONOO^-$, which are capable of causing strand breaks in chromatin (Tanaka et al., 2005).

Cell swelling due to cytoplasmic edema is one of the earliest observable morphological changes in necrotic cells (Calvert and Zhang, 2005). The overactivation of NMDA and AMPA receptors caused by glutamate exitotoxicity leads to rapid Na^+ and Cl^- influx during energy failure and contributes to edema through altered cellular osmotic balance (Dirnagl, Iadecola, and Moskowitz, 1999). Altered osmotic balance caused by Ca^{2+}, Cl^-, and Na^+ influx then causes extracellular water to enter the cytosol in large quantities (Blomgren, Leist, and Groc, 2007). Cells expanding due to edema eventually explode and fragments are released into the intracellular matrix. The release of cell fragments and intracellular content into the matrix triggers the inflammatory response (Chowdhury, Tharakan and Bhat, 2006).

Pro-inflammatory cytokines are released from neutrophils rapidly in response to injury, activating microglia (the resident macrophages of the brain) and causing the expression of endothelial adhesion molecules, promoting leukocyte infiltration into the damaged region (Wang et al., 2002). Once microglia are activated, they have the potential to cause damage to viable cells not damaged by initially by HI through the release of neurotoxic substances including ROS, NO, and pro-inflammatory cytokines (Lai and Todd, 2006). As a result of their neurotoxic properties, the overactivity of microglia in response to injury can severely exacerbate brain damage in response to inflammation.

1.2.3. Apoptotic cell death

In cells that experience energy loss capable of causing mitochondrial failure, but not necrosis, or cells that receive molecular death signals initiated by HI, apoptotic death mechanisms are activated, causing delayed cell death up until approximately 7 days after the insult (Gunn and Thoresen, 2006). In contrast to necrosis, apoptosis requires energy in the form of ATP to produce the proteins required for apoptotic signalling. The morphological characteristics of apoptotic cells are distinct from healthy and necrotic cells as apoptotic cells demonstrate membrane blebbing, nuclear fragmentation, and chromatin break-down (Giffard and Swanson, 2005). The final result of apoptotic processes is cellular disassembly followed by digestion of cellular fragments by macrophages (Banasiak, Xia, and Haddad, 2000). Because of the energy-requiring processes necessary for apoptosis, the apoptotic cascade can be modulated and influenced such that many cells may be salvaged following HI (Edwards et al., 1995).

There are two pathways of apoptosis that will be addressed in the current paper. The first is the extrinsic apoptotic pathway which involves death ligands interacting with membrane receptors to promote apoptotic death. Examples of ligands that act as death signals include tumour necrosis factor-alpha (TNF-α) and Fas Ligand (FasL: Harper et al., 2003). These ligands go on to activate signal transduction pathways responsible for the execution of apoptosis. The action of these pathways culminates in

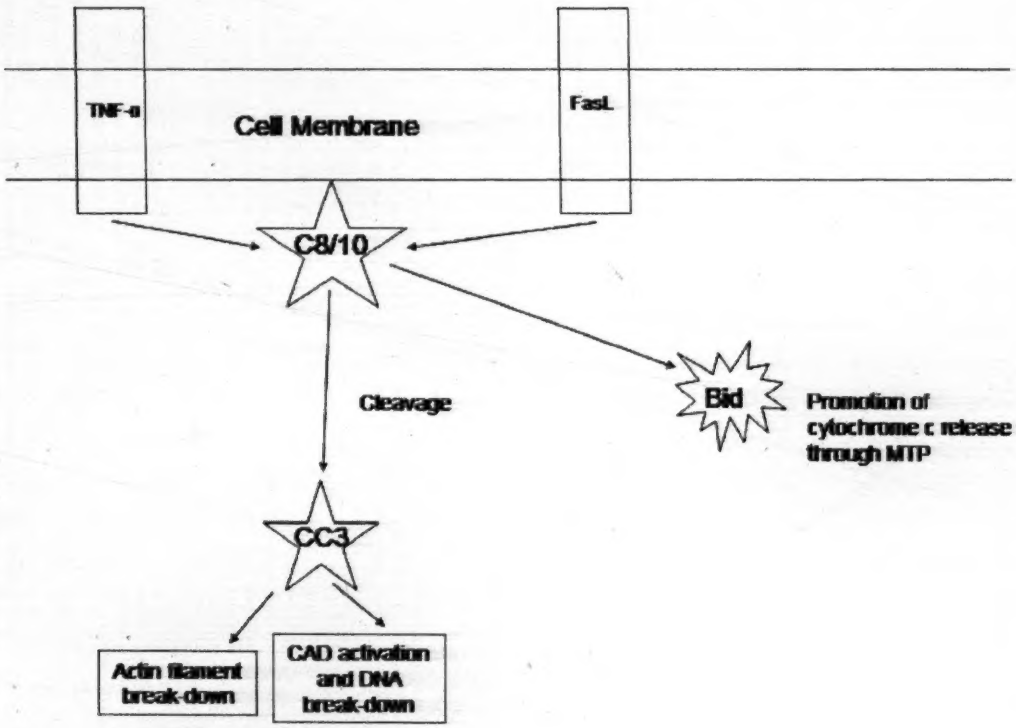

Figure 1-2. Signalling pathways in extrinsic apoptosis.

The extrinsic pathway of apoptosis is stimulated by the binding of cell death ligands including TNF-α and FasL to receptors on the cell membrane. Caspase 8 and 10 then stimulate cleavage of caspase-3 or the activation of Bcl interacting domain (Bid). Bid contributes to the opening of the mitochondrial transition pore through its action on the proteins bax and bak further downstream in the apoptotic cascade. Figure adapted from Huerta et al., (2007).

the cleavage of effector caspases that finalize the apoptotic process (Figure 1-2: Calvert and Zhang, 2005).

The second major pathway of apoptosis is the intrinsic apoptotic pathway (Figure 1-3). The intrinsic apoptotic pathway involves the opening of the mitochondrial transition pore (MTP) leading to the release of cyt c which ultimately activates cysteine proteases responsible for break-down of DNA as well as the nuclear and cellular membranes (Martinou and Youle, 2006). Upstream of cyt c release, anti-apoptotic and pro-apoptotic proteins are released as a result of either death signals or the action of survival factors on the cell (Banasiak et al., 2000). Different members of the B-cell lymphoma 2 (bcl-2) family of proteins have either pro-apoptotic or anti-apoptotic effects on the mitochondria (Munoz-Pinedo, 2006). Bcl-2 and bcl-xl act as anti-apoptotic stimuli by preventing MTP opening while the pro-apoptotic proteins bax and bak have the ability to increase mitochondrial membrane ion permeability and to promote MTP opening (Hu et al., 2003). If signalling via pro-apoptotic proteins is made prominent, the MTP will be stimulated into opening and cyt c release will occur through the open MTP along with other proteins that further the apoptotic cascade (Ravagnan, Roumier, and Kroemer, 2002).

Once cyt c is released from the MTP, it goes on to join a large molecular complex known as the apoptosome. Cyt c first binds to pro-caspase-9 (which becomes cleaved upon binding to the rest of the apoptosome complex), and apoptotic protease activating factor-1 (apaf-1) in the presence of ATP to form the completed apoptosome (Ravagnan, Roumier, and Kroemer, 2002). The apoptosome continues the apoptotic cascade, functioning as an activation complex to cleave pro-caspase-3

and pro-caspase-6, forming activated (cleaved) caspase-3 (CC3) and cleaved caspase-6 (CC6: Estaquier and Arnoult, 2007). Once activated, CC3 disassembles actin filaments, causing the cell membrane to bleb and fail structurally such that the apoptotic cell develops its characteristic wrinkled morphology (Chang and Yang, 2000). As well, DNA fragmentation and chromatin condensation occur due to CC3's activation of caspase activated DNase (CAD) through deactivation of CAD's inhibitor (inhibitor of CAD), leading to the break-down of the nuclear membrane (Blomgren, Leist, and Groc, 2007). The nucleus itself is broken up in the final stages of apoptosis by CC6, which cleaves lamins, the scaffold proteins that maintain the structure of the nuclear envelope (Chang and Yang, 2000).

1.3. Secondary energy failure following hypoxic-ischemia

Levels of high energy phosphates (ATP and PCr) have been observed to recover shortly after HI in rodent models due to the brain's return to normal oxidative metabolism and circulation following HI, a period known as the reperfusion period (Gunn and Thoresen, 2006). Following the reperfusion period there is a period of recovery during which levels of ATP and PCr remain constant (Guan et al., 2003). However, after the stabilization of ATP and PCr levels, a secondary drop occurs after the recovery period (Gunn and Thoresen, 2006). The delayed drop in ATP and PCr levels has been labelled secondary energy failure (SEF) and it has been observed in both human and animal studies (Gunn and Thoresen, 2006). In magnetic resonance spectroscopy (MRS) studies, post-HI drops in ATP and PCr have been shown to occur in human neonates suspected of being exposed to HI insults. These neonates demonstrate a secondary drop in ATP and PCr 24-48 hours after HI (Vannucci,

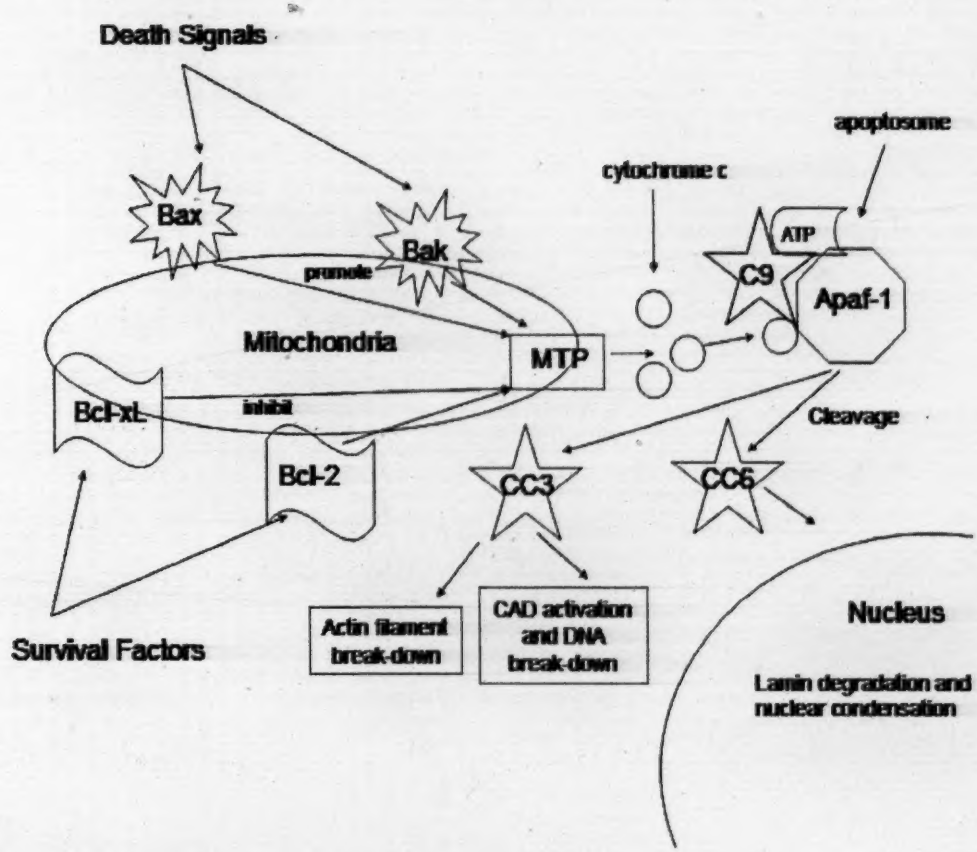

Figure 1-3. Signalling pathways in intrinsic apoptosis.

In the intrinsic pathway of apoptosis, survival factors cause bcl-2 and bcl-xl to prevent the MTP from opening in the mitochondrial membrane. In contrast, death stimuli promote the binding of the proteins bax and bak which open the MTP and allow cyt c to escape the mitochondria, forming the apoptosome with caspase-9, apaf-1 and ATP. The apoptosome goes on to cleave caspase-3 and caspase-6, enabling these proteins to disassemble DNA and lipid membranes. Figure adapted from Huerta et al., (2007).

Towfighi, and Vannucci, 2004). In the neonatal rat, levels of ATP have been observed to undergo a secondary decrease at approximately 72 hours (Armstrong and Yager, Unpublished: Figure 1-4).

The severity of SEF, as measured by the extent of delayed ATP and PCr decrease, is correlated with the degree of brain damage, with larger drops in ATP and PCr being correlated with more severe brain damage (Roth et al., 1997). Due to the delayed nature of the ATP/PCr drop, the period between reperfusion and SEF provides an opportunity to provide neuroprotective therapy and salvage cells that would otherwise die (O'Brien et al., 2006). Because of the close correlation between SEF severity and outcome, treatments that increase the availability of ATP and PCr after HI should reduce the extent of damage by lessening SEF (Erecinska, Thoresen, and Silver, 2003). These treatments are also most effective when administered as soon as possible following HI, since the changes in ATP and PCr levels that lead to SEF can be reversed more easily early on in the reperfusion period (Gunn and Thoresen, 2006).

1.4. Post-hypoxic-ischemic hypothermia

1.4.1. Hypothermia as a neuroprotective treatment

Hypothermia has been used successfully in both laboratory and clinical trials as a treatment for HI (Shankaran et al., 2002). Despite harmful side-effects that may result from hypothermia including shivering (which reverses the effects of hypothermia while core temperature rises), apnea, and frostbite when hypothermia is deep, hypothermia became of interest in laboratory studies during the 1980s with demonstration of the effectiveness of mild hypothermia in animal models of adult

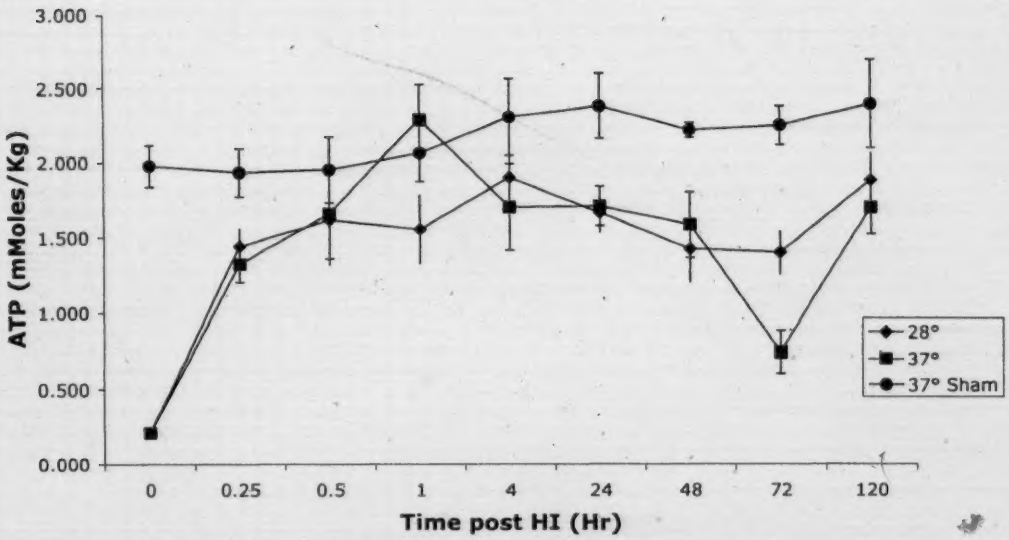

Figure 1-4. Time-dependent changes in ATP and PCr in PND 7 rats following HI.

Data from Armstrong and Yager (unpublished) illustrating the secondary decline in ATP at 72 hours post HI in rat pups. HI-treated animals in the 37 °C group had a significantly lower concentration of ATP than animals in the Sham group. Used with permission.

cerebral ischemia (Thoresen and Whitelaw, 2005). Since the initial studies were published, hypothermia has been used effectively to decrease damage in both neonatal and adult animal models of ischemic brain injury (Wagner et al., 1999).

In clinical hypothermia trials conducted with human neonates, some success has been observed using hypothermia as a treatment for HI. For example, two large-scale multi-centre clinical trials have shown that hypothermia is effective at reducing the impact of mild HI insults (Gluckman et al., 2005), and that hypothermia can be applied without risk of harmful long-term side-effects (Shankaran et al., 2002). However, the mechanisms of hypothermia, its most beneficial co-treatments, and the optimal conditions necessary to maximize neuroprotection using hypothermia have not yet been elucidated (Gunn and Thoresen, 2006).

Despite a lack of specific knowledge concerning the application of hypothermia in individual cases and the underlying mechanisms, some strategies to maximize the effectiveness of hypothermia have been developed. For example, either systemic or head-only hypothermia applied immediately following cerebral ischemia is more effective than hypothermia applied after a delay, with longer delays leading to less improvement in outcome (Gunn and Thoresen, 2006). Research has also shown that providing hypothermia for long periods of time (over 24 hours) is more effective than providing hypothermia for shorter periods such as 3 hours (Ohmura et al., 2005). Shorter periods of hypothermia have been observed to delay apoptotic death rather than provide long-term neuroprotection (Bona et al., 1998). As well, different effects can be produced by either mild hypothermia (a drop of up to 3 °C), moderate hypothermia (a drop of 5 °C to 10 °C), or severe hypothermia (a drop of more than 10

°C), with deeper hypothermia increasing side-effects while enhancing cell survival (Gunn and Thoresen, 2006).

Some of the suggested mechanisms of hypothermia include enhanced energy recovery (Erecinska, Thoresen, and Silver, 2003), delay and prevention of inflammatory processes, reduction of free radical production (Calvert and Zhang, 2005), prevention of seizures (Thoresen and Whitelaw, 2005), and the safe return of brain pH to normal physiological levels (approximately 7.0) after HI (Erecinska, Thoresen, and Silver, 2003). Also, improvement in the rate of protein synthesis in tissue treated with hypothermia has been reported *in vitro* after HI despite the fact that inflammatory mediators and apoptotic signaling mechanisms are downregulated (Berger and Garnier, 1999). Hypothermia has also been observed to reduce tissue edema and to protect the integrity of the blood-brain barrier (BBB) later on in the post-HI injury process (Inamasu et al., 2000).

1.4.2. Neuroprotective mechanisms of hypothermia

Arguably, the most important neuroprotective mechanism of hypothermia is energy recovery (Erecinska, Silver, and Thoresen, 2003; Gunn and Thoresen, 2006; Perlman, 2006). Hypothermia reduces ATP consumption, leading to enhanced energy recovery resulting from increased ATP and PCr levels to reduce the extent of HI damage (Kimura et al., 2002). For example, increased ATP availability during the reperfusion period has been correlated with less severe SEF and better outcome following HI (Erecinska, Silver, and Thoresen, 2003).

An effect of the immediate application of hypothermia after HI is reduction of excitotoxic glutamate levels in the post-HI period (Perlman, 2006). The global effect

of the increased ATP levels that result from applying hypothermia immediately after HI is the prevention of continued AD caused by glutamate release (Berger et al., 2004). In the synaptic cleft, glutamate re-uptake is improved since ATP levels are maintained, allowing better function of glutamate transporters and removal of glutamate before excitotoxic effects can occur (Asai et al., 2000).

Hypothermia also significantly reduces the production of ROS (Hammer and Krieger, 2003). One of the factors affecting the rate of ROS generation following HI is the mitochondrial membrane potential which is influenced by the availability of ATP and PCr (Meyer et al., 2006). The greater availability of ATP resulting from hypothermia helps maintain mitochondrial membrane potential and prevents ROS formation. As well, hypothermia reduces the activity of $OH^{\cdot}$ radicals following HI, although the mechanisms have not yet been determined (Hashimoto, Yonetani, and Nakamura, 2003).

Hypothermia has also been shown to reduce the impact of inflammatory processes following HI. Specifically, hypothermia significantly decreased the ischemia-induced release of cytokines such as TNF-α following cerebral ischemia (Yenari and Han, 2006). Hypothermia also reduces the impact of inflammation by reducing the accumulation of harmful neutrophil (white blood cells that move into a damaged brain region from the blood stream: Inamasu et al., 2000), and leukocyte infiltration through downregulation of intercellular adhesion molecule-1 (necessary for leukocyte infiltration into the brain) following adult stroke (Deng et al., 2003). As well, microglia activity has been shown to be decreased in response to hypothermia (Wang et al., 2002). The result of hypothermia treatment is greatly reduced

cytotoxicity in the post-HI period, leading to increased survival of potentially viable cells following HI (Yenari and Han, 2006).

1.5. Enhancing the neuroprotective effects of hypothermia

Despite hypothermia's myriad of effects on pathological processes, only 15% of infants treated with hypothermia in clinical trials following mild HI showed improved outcome compared to infants treated with pharmacological post-HI treatments (Gunn and Thoresen, 2006). In light of hypothermia's mediocre performance in clinical trials and since few stand-alone pharmacological treatments have been successful for HI, combination strategies need to be investigated as the next logical step in improving hypothermia treatment for HI.

Studies combining hypothermia with pharmacological treatments have shown moderate success in laboratory trials thus far and have focused on a wide-array of mechanisms to do so. Drugs used in combination with hypothermia for the treatment of neonatal HI include N-acetylcysteine (a free radical scavenger: Jatana et al., 2006), xenon (an anesthetic that acts as a noncompetitive antagonist of NMDA receptors: Ma et al., 2005), MK-801 (a NMDA antagonist: Alkan et al., 2001), and dipyrone (an anti-inflammatory drug: Coimbra et al., 1996).

Although hypothermia combination treatments have seen shown to improve neurological and long-term behavioural outcome after HI in animal models, many potential treatments such as MK-801 and dipyrone are not practical in clinical settings as they produce harmful side-effects making them undesirable for use in humans (Gunn and Thoresen, 2006). In addition to the issues of safety and side-effects that surround potential co-treatments, the majority of treatments that perform well in

laboratory settings have shown little value in clinical trials (Ikonomidou and Turski, 2002). One of the problems of poor clinical drug translation is attributed to the difficulty of treatment timing in human neonates and the difficulty involved with determining whether or not an infant has suffered an HI insult (Vannucci and Perlman, 1997).

1.6. Creatine as a hypothermia co-treatment

1.6.1. Creatine synthesis and metabolism

Administering creatine (Cr) as a co-treatment with hypothermia could improve the recovery of energy in brain cells following HI since Cr regulates ATP and adenosine diphosphate (ADP) phosphate cycling and Cr has been shown to be effective when administered prior to HI (Holtzman et al., 1998). Cr has the potential to be an effective co-treatment for hypothermia due to its minimal side-effects, and reports have shown it to be very safe in a variety of applications in humans (Bohnhorst et al., 2004). For instance, Cr is often used to increase cellular energy reserves in muscle and is used regularly by athletes performing demanding anaerobic activities (Wilkinson et al., 2006).

Cr is an endogenous compound that is ingested regularly in meat by many mammals and Cr is also synthesized in the liver, kidneys, and heart (Wyss and Kaddurah-Daouk, 2000). Cr is derived from reactions catalyzed by the enzyme L-arginine:glycine amidinotransferase (AGAT) that transfers an amidino group from arginine to glycine yielding L-ornithine and guanidinoacetic acid (GAA). GAA is then methylated at the amidino group by S-adenosyl-L-methionine:N-guanidinoacetate (GAMT), resulting in Cr formation (Figure 1-5: Wyss and Kaddurah-Daouk, 2000).

Cr is broken down into its metabolite, creatinine, due to break-down caused by creatine amidinohydrolase which occurs at a rate of approximately 1.0% per day under normal physiological conditions (Wyss and Kaddurah-Daouk, 2000).

Na^+- and Cl^--dependent membrane-spanning BBB Cr transporters are responsible for Cr's entry into the brain (Wyss and Kaddurah-Daouk, 2000). After being injected subcutaneously or by intraperitoneal injection, Cr enters the brain by means of Cr transporters found in brain capillary endothelial cells that mediate the supply of Cr passing through the BBB (Ohtsuki et al., 2004). Blood-borne Cr is then taken up into neurons and glia by the Na^+- and Cl^--dependent transporters in the cell membrane (Sestili et al., 2006). However, endothelial Cr transporters can be easily saturated even by oral Cr administration (Ohtsuki, 2002). The result is a variable time-lag between Cr injection and uptake into brain cells.

1.6.2. Neuroprotective effects of creatine

Cr influences a variety of cell death mechanisms. However, the primary mechanism of Cr is suggested to be energy recovery (Berger et al., 2004). Cr acts as an energy buffer at the molecular level, supplying energy in the form of free phosphate groups (Pi) to ADP when ATP is depleted (Wyss and Kaddurah-Daouk, 2000). Cr accomplishes its energy buffering role by being phosphorylated into PCr by Cr kinase (CK) which is more common in cells that have high energy demands (Holtzman et al., 1998). CK in the brain comes in the form of brain CK and mitochondrial CK (MiCK: Manos and Bryan, 1993).

During the reperfusion period after HI, Cr helps to maintain ATP levels by acting as an energy buffer and adding Pi to ADP and adenosine monophosphate (AMP:

Holtzman et al., 1998). During HI, levels of PCr decrease rapidly in the brain once oxygen and blood flow decrease as PCr compensates for the lack of ATP in the absence of oxidative metabolism (Yager, Brucklacher and Vannucci, 1992). Therefore, higher levels of Cr in the brain can help preserve cellular functions during HI and improve post-HI outcome. Ultimately, maintaining higher ATP levels with Cr supplementation has been correlated with reduced activity of pathological processes and the loss of fewer cells via apoptosis (Zhu et al., 2004).

Several studies have demonstrated Cr's effectiveness as a neuroprotective agent. Work by Holtzman et al., (1998) in the post-natal day (PND) 7 rat showed increased PCr and decreased infarct volume with Cr supplementation. A more recent study by Adcock et al. (2002) in PND 10 rats showed, using MRS, that levels of both ATP and PCr were significantly increased following injury by pre-HI Cr supplementation. Work by Vannucci, Towfighi, and Vannucci (2004) also showed that infarct size was smaller after HI when physiological levels of Cr were high, as more PCr was available to phosphorylate ADP following injury. Cr has also been demonstrated to provide pre-ischemic neuroprotection in adult mice along with increases in PCr and ATP (Prass et al., 2006).

Despite being studied almost exlusively as a pre-HI treatment, Cr has the potential to be effective following HI as SEF occurs due to a decrease in ATP levels resulting in continuing cell death after HI (Vannucci and Hagberg, 2004). By increasing ATP's availability through enlarging the pool of Cr in the brain, Cr could potentially reduce the severity of SEF. In addition to decreasing the severity of SEF,

Cr has been found to aid in the recovery of protein synthesis *in vitro*, results that have been proposed to translate *in vivo* (Berger et al., 2004).

1.6.3. Creatine and mitochondrial function

Cr is also important as a Pi carrier in mitochondrial respiration due to the mitochondria being the site of ATP in the cell. Cr is used as a spatial energy buffer to ferry Pi molecules to and from the mitochondria from the cytoplasm in the form of PCr (Brewer and Walliman, 2000). The increased availability of Pi by means of Cr also allows ADP and AMP to be phosphorylated into ATP more rapidly. As a result, increased levels of Cr following HI can preserve mitochondrial function during energy failure, allowing ATP to be produced at an increased rate.

Mitochondrial swelling as a result of energy failure contributes to MTP opening and cyt c release signaling apoptosis (Bernardi et al., 2006). Mitochondrial swelling during and after HI is caused by an increased influx of cellular Ca^{2+}, and enhanced PCr may provide mitochondrial membrane ion ATPases with the energy necessary to prevent mitochondrial swelling from occurring (Brustovetsky, Brustovetsky, and Dubinsky, 2001). An increase in PCr in the mitochondria has been shown to result in up to a 20% decrease in mitochondrial swelling, reducing the severity of processes that contribute to apoptosis (Brustovetsky, Brustovetsky, and Dubinsky, 2001). The presence of excess Cr in the mitochondria can also block the MTP from opening by forming an octomer with MiCK. The result of octomer production is the blockage of the MTP, preventing cyt c release and apoptosis (Klivenyi et al., 2004).

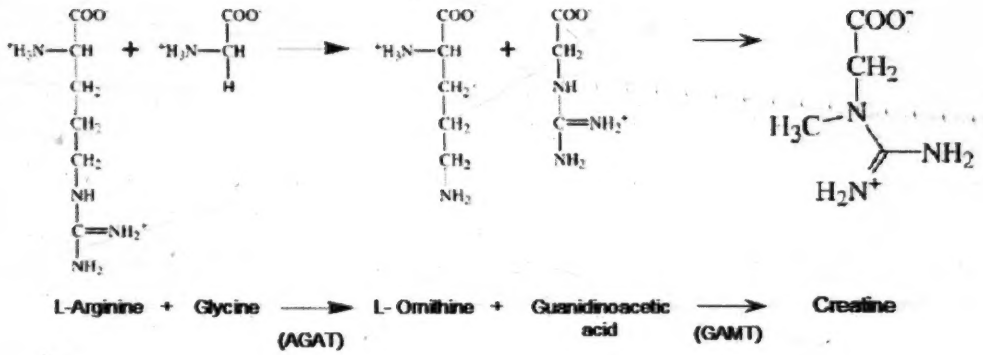

Figure 1-5. Endogenous synthesis of Cr.

Cr is synthesized by a reaction between the amino acids arginine and glycine catalyzed by AGAT which transfers an amidino group to glycine. L-orinithine and GAA are produced as a result. GAA is then methylated at the amidino group to yield Cr. Figure adapted from Wyss and Kaddurah-Daouk, (2000).

1.6.4. Creatine and reactive oxygen species

In addition to preventing mitochondrial dysfunction, Cr has been found to reduce ROS production and activity. Work by Sestili et al., (2006) has shown that Cr can protect cells from ROS *in vitro*. The mechanism by which Cr exerts these effects is through reacting directly with ROS in the cytosol (Wyss and Kaddurah-Daouk, 2000). Very high concentrations of Cr have been found to neutralize ROS in *in vitro* experiments by attracting negatively charged ROS and Cr may produce similar effects *in vivo* (Lawler et al., 2002). For example, the positive charge of the N-methyl group on the Cr molecule attracts negatively charged ROS including OH^-, $ONOO^-$, and O_2^-, forming compounds that are no longer harmful (Sestili et al., 2006). Alternatively, Cr's ability to increase energy recovery and ATP availability may prevent the exhaustion of ROS scavengers in a similar fashion to hypothermia, reducing the amount of cellular damage caused by ROS (Meyer et al., 2006).

1.7. In vivo animal models of neonatal hypoxic-ischemic brain damage

A variety of *in vivo* neonatal HI models have been developed to serve different needs in HI research. Some of the variables affecting animal model selection for a particular experiment include cost, ease of use, including the application of surgical and analytical methods, and similarity to human neonates based on the degree to which each animal is either altricial or precocial (Erecinska, Silver, and Thoresen, 2003). Some of the most commonly used animals are rodents such as the rat, mouse, and gerbil.

In experiments requiring larger animal models, sheep and piglets are often used. In the piglet model, the relatively large size of the animal and its similar

precocial condition to human neonates at birth make it an ideal subject for use in post-HI electroencephalography (Björkman et al., 2006). The piglet also provides a larger animal for more complex invasive experimental procedures including precise temperature monitoring and physiological analysis.

In contrast to piglets, rats are born more altricial than humans and they are used several days after birth as a result, typically between PND 7 and PND 10 (Gunn and Thoresen, 2006). Rat models have the advantage of being very efficient for use in experimental models due to their small size, low cost, and the wealth of data accumulated in rat studies (Vannucci and Vannucci, 2005). Rats are also highly adaptable for behavioural testing following injury while their brains are relatively small and well characterized for histology (Kolb and Whishaw, 2003).

In the adult rat, one of the original models of HI brain damage is the Levine model (Levine, 1960). Both carotid artery ligation and hypoxia are needed to simulate natural HI damage effectively and they are used in concert with each other (Comi et al., 2004). In the Levine model, unilateral common carotid artery ligation is followed by limited inspiration of an 8% O_2-balanced nitrogen mixture for up to 3 hours depending on the severity of injury required in a particular study (Vannucci et al., 1999).

The Levine model was adapted to the rat pup and served as the basis for the later Rice-Vannucci model utilized in the current study (Rice, Vannucci, and Brierly, 1981). As the rat is more altricial than larger animals the age that rats are exposed to HI is important depending on the goals of the experiment. PND 7-8 rats are employed

in the Rice-Vannucci model as they are developmentally similar to 32-34 week old human fetuses (Vannucci et al., 1999).

Similar to the Levine model, the method of producing HI in rat pups begins with ligation of the carotid artery (typically on the right side of the animal). Following a recovery period of 1 to 2 hours spent with the dam, animals are exposed to 8% O_2-balanced nitrogen in an enclosed environment for up to 3.5 hours at which time appreciable mortality begins to occur (Rice, Vannucci, and Brierley, 1981). The time in hypoxia can be manipulated to produce varying severities of damage, with longer times in hypoxia and greater humidity causing more severe damage. Damage observed after hypoxia is largely conserved to the ligated hemisphere and it is particularly prominent in the cortex, white matter tracts, and deep gray matter structures such as the basal ganglia (Vannucci et al., 1999).

1.8. Hypothesis

The objective of the study described in this thesis was to determine if post-HI Cr or a combination treatment of Cr and hypothermia would provide greater neuroprotection than hypothermia alone. Our hypothesis was that Cr supplementation would enhance hypothermia treatment and result in greater neuroprotection after neonatal HI as observed in the form of brain infarct volume after injury and the decreased presence of apoptotic markers.

CHAPTER 2: MATERIALS AND METHODS

2.1. Experimental animals

This research protocol was approved by the Health Science Animal Policy and Welfare Committee of the University of Alberta. The animals used were Long-Evans rat pups bred at the University of Alberta, Edmonton, Canada. All dams were housed in standard cages and had free access to food and water *ad libitum*. All animals used in the study were maintained in a thermo-controlled room kept at 20 ^{0}C, and exposed to 12 hour on/off lighting. Rat pups were born vaginally and litters were culled to 10 pups each on the first day of birth, resulting in an equal distribution of male and female pups.

Five groups of rat pups were utilized in the low-dose (3 mg/kg) study (Table 2-1) while six groups were used in the high-dose (3 g/kg) study (Table 2-2). The vehicle normothermic (VN) group consisted of normthermic animals injected with normal saline; the Cr normothermic (CN) group consisted of normothermic animals injected with Cr; while the vehicle hypothermic (VH) group consisted of hypothermic animals injected with normal saline. The combination or Cr hypothermic (CH) group consisted of hypothermic animals given Cr. Animals exposed to HI and left with the dam made up the HI control group (HIC). As well, a group of animals were left untreated and they were referred to as sham (S) animals.

Injection	Temp	Group	Number
Creatine	37 ^{0}C	CN	18
Creatine	28 ^{0}C	CH	18
Veh	37 ^{0}C	VN	20
Veh	28 ^{0}C	VH	21
None	NA	HIC	9
		TOTAL	108

Table 2-1 Treatment groups used in the low-dose 3 mg/kg study.

Injection	Temp	Group	Number
Creatine	37 ^{0}C	CN	28
Creatine	28 ^{0}C	CH	23
Veh	37 ^{0}C	VN	28
Veh	28 ^{0}C	VH	20
None	NA	S	30
None	NA	HIC	21
		TOTAL	150

Table 2-2 Treatment groups used in the high-dose 3 g/kg study.

2.2. Induction of hypoxic-ischemia

PND 7 Long-Evans rat pups underwent a carotid artery ligation based on the Rice-Vannucci rat HI model (Rice, Vannucci, and Brierly, 1981). After being weighed, sexed, and randomized to groups each animal was anesthetized using halothane balanced with 30% O_2-balanced nitrogen at 4% induction prior to surgery followed by 1% halothane maintenance. A midline neck incision was made and the right common carotid artery was identified, and separated from the vagal nerve. The right carotid artery was then double ligated using 3-0 surgical silk, and cut between ligations. Afterwards, the wound was closed with 3-0 surgical silk and the pups were allowed to recover with their dam for 2 hours prior to HI.

HI was induced by placing animals in 500 ml glass jars (maximum 3 per jar) through which 8% oxygen-balanced nitrogen was vented. Thermoregulation was maintained by placing the jars in heated water-baths at 36.5 +/- 0.5 ^{0}C.. Rat pups were exposed to HI conditions for 90 minutes.

2.3. Low-dose injection protocol

A dose of 3 mg/kg was used prior to the high (3 g/kg) dose of Cr. Surgery and HI procedures were the same at both injection concentrations. Induction of hypothermia and normothermia were similar as well, with the exception of glucose infusion. Both hypothermic and normothermic animals were infused with a 15% glucose solution in 0.9% saline. However, hypothermic animals received glucose at a rate of 8.33 μl/hour, while normothermic animals received glucose at a rate of 25

µl/hour to compensate for the difference in metabolism between hypothermic and normothermic animals.

Following the 24-hour hypothermic or normothermic period, Cr (3 mg/kg) or normal saline (0.9%) was injected subcutaneously into the medial dorsal scruff repeatedly and every 24 hours for 5 consecutive days. The amount of Cr given in the injection was increased as the animals grew such that the volume was maintained at 100 µl while a 3 mg/kg dose was maintained. Animals were sacrificed on PND 14, 2 days following the 5 consecutive days of Cr injection. Brains were removed and fixed by means of immersion in a mixture of formaldehyde, acetic acid and methanol (FAM). Damage ranking was performed on brains once all brains were removed as described in section 2.5. The procedure for paraffin embedding is described below in section 2.6.

2.4. Preliminary studies

To determine the effect of Cr administration on glucose metabolism and core temperature, animals were fitted with surgical tubing (PE-10) such that glucose or combined glucose/Cr (3 g/kg) solutions could be infused subcutaneously. The tubing was secured with Krazy Glue, and attached to 1.0 ml syringes connected to a Harvard bee-hive syringe pump. The volume of solution administered was 2.4 ml in each group over the 24-hour period.

Cr injection volume was increased such that the concentration of Cr was kept at or below 30 mg/ml by increasing injection volume for ease of dissolution. The Cr solution was heated to approximately 50 ^{0}C and stirred until dissolved. The solution was allowed to cool to a temperature of approximately 25 ^{0}C or less before injection.

Glucose solutions and glucose/Cr solutions were administered at a rate of 100 µl/hour over 24 hours. Animals were injected for 4 consecutive days following hypothermia. Injections were administered in 8-hour intervals beginning 8 hours after hypothermia. Injections of either Cr (3 g/kg, Sigma Chemical) or saline (0.9%) were given subcutaneously in the middle of the back using a 29-gauge needle at a concentration of no more than 30 mg/ml.

Previous investigations have shown a Pearson's R correlation between brain and rectal temperatures to be approximately 0.97 in a PND 7 rat pup model (Ohmura et al., 2005). These findings indicate that monitoring body temperature to determine brain cooling is effective and necessary to gauge temperature-related physiological effects. In the current study, water bath temperatures were maintained at 36.5 +/- 0.5 ^{0}C in normothermic conditions and 27.5 +/- 0.5 ^{0}C under hypothermic conditions. Previous work has shown that exposing PND 7 rats to a 28 ^{0}C environment results in a rectal temperature of approximately 31-32 ^{0}C in a rat pup HI model, a temperature shown to be neuroprotective (Yager and Asselin, 1999).

To confirm that these temperatures were achieved in experimental animals, rectal thermometers were placed 1.5 cm into the anus to record core temperature. Three animals per group were used to determine mean temperatures in each of the 4 treatment groups (VN, VH, CN, and CH) during the 24 hour period of hypothermia or normothermia. Temperature data were recorded in 10-minute intervals using a custom-made software program on a PC. Animals used for measuring core temperature were sacrificed immediately following the 24-hour period of hypothermia/normothermia and blood glucose levels were analyzed as follows.

Given that the rat pups were to be maintained independently from their dams for 24 hours post-HI to induce hypothermia, preliminary studies were undertaken to ensure the adequacy and consistency of glucose concentrations in each group. Rat pups from the above temperature procedures were sacrificed at the end of the hypothermia or normothermia by means of decapitation. Blood samples were obtained from severed neck vessels and analyzed for glucose concentrations using a One Touch Ultra glucose meter. To determine glucose infusion volumes that would prevent hypoglycemia or hyperglycemia from occurring in the animals, infusions of 15%, 3.45%, 0.86%, 0.75%, 0.50%, and 0.30% glucose were used in hypothermic animals while infusions of 15%, 3.75%, and 3.25% were used in normothermic animals. Analysis of glucose data suggested that animals in the hypothermic groups required a glucose solution at a concentration of 0.30% due to decreased core temperature during hypothermia while normothermic animals required a 3.25% glucose infusion.

2.5. Ranking of damage

All brains collected in the experiment were ranked visually based on the relative severity of damage observed by an observer blind to treatment groups. Brains that had suffered more visible damage in the right hemisphere were given a higher score while brains appearing less damaged were given a lower score (Figure 2-1). A brain appearing undamaged received a rank of 0 and undamaged brains served as a baseline for rank scoring.

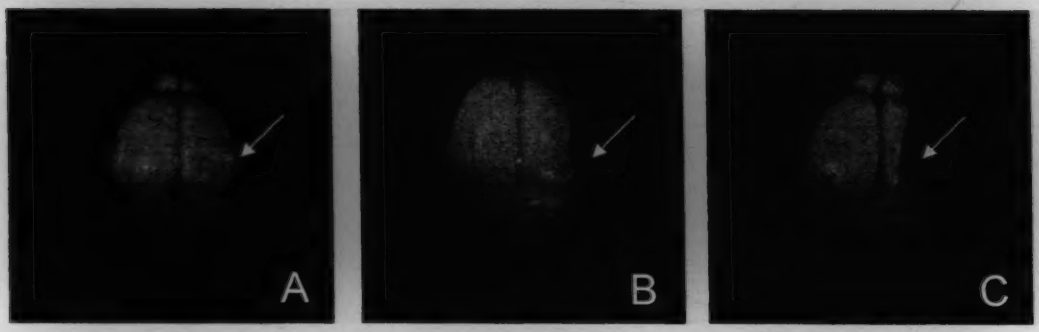

Figure 2-1. Lesion severity in PND 14 rats.

Lesioned hemisphere indicated by arrow. Damage was classified as being mild (A), moderate (B), or severe (C). Animals with mild damage typically showed small focal lesions and/or cortical asymmetry. Animals with moderate damage had larger global lesions that visibly reduced the size of the ipsilateral hemisphere. In the severely damaged animals, the majority of the damaged hemisphere was lost.

2.6. Animal sacrifice

Animals were sacrificed on PND 14, 7 days following HI. Halothane gas (5%) was administered until animals were no longer responsive to tactile stimulation such that decapitation could be performed without pain. Brains were removed and immersed in FAM solution which was changed to 70% ethanol after 48 hours. Whole brains were then embedded using paraffin wax for sectioning.

2.7. Tissue sectioning

Tissue sectioning was performed using a microtome and sections were floated on a waterbath at a temperature of 54 ^{0}C. Sectioning for volumetric analysis began prior to the splenium of the corpus callosum and ended at the genu of the corpus callosum. Coronal sections 6 μm thick were taken every .5 mm. Sections for immunohistochemistry staining were taken such that the hippocampus, striatum, cortex, thalamus, and hypothalamus could be examined in posterior, medial, and anterior sections. Prior to staining, sections were baked at 52 ^{0}C for 60 minutes to ensure proper adhesion to slides.

2.8. Hematoxylin and eosin staining

Sections were stained using Harris Hematoxylin and Working Eosin solution. Sections were deparaffinized by immersion twice in xylene for 5 minutes followed by 1 minute in 100% ethanol and 1 minute in 95% ethanol. After deparaffinization, slides were placed in hematoxylin for 3 minutes and rinsed using distilled water. Sections were then dipped in acid alcohol 4 times (1 second per dip), rinsed in distilled water, and placed in working eosin solution for 10 seconds while being agitated.

Tissue was dehydrated by placement in 95% ethanol for 2 minutes, 100% ethanol for 2 minutes, and xylene for 2 minutes before being coverslipped with cytoseal.

2.9. Analysis of infarct volume

To quantify infarct volume, Hematoxylin and Eosin (H and E) stained slides were photomicrographed using Spot Advanced imaging software v.4.5. Images were then imported into National Institutes of Health (NIH) imageJ v.1.37p for analysis. Photomicrographs of each coronal section were analyzed to determine infarct area by subtracting the area of the lesioned hemisphere from the undamaged hemisphere. Total infarct volume was then calculated using GraphPad Prism v. 4.00 using an area-under curve measurement. Means from each group were then compared using a one-way analysis of variance (ANOVA).

2.10. White matter analysis

Colour-enhanced photomicrographs (with red light reduced by 80% using Spot Advanced v.4.5.) of H and E stained tissue were used to measure the thickness of white matter structures. External capsule boundaries were identified using *The Rat Brain in Stereotaxic Coordinates: Second Edition* (Paxinos and Watson, 1998) and measured using NIH imageJ v.1.37p. Posterior external capsule was measured at approximately -3.60 mm bregma (plate 32), while anterior external capsule was measured at approximately 0.48 mm bregma (plate 16: Paxinos and Watson, 1998). The thickness of the medial external capsule was measured in both posterior and anterior sections (Figure 2-2). All measurements were made using ImageJ v.1.37p software.

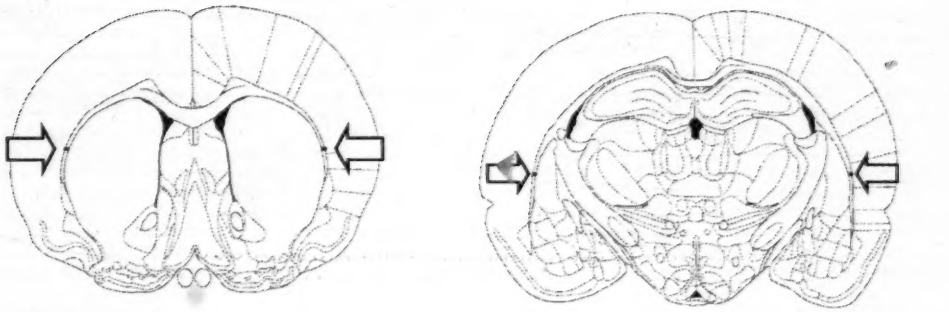

Figure 2-2. External capsule thickness.

The thickness of the external capsule was measured at the medial caudate putamen in (A) anterior sections and (B) posterior sections of the brain. Anatomical landmarks used for measurements were made using Figure 32 (A) and Figure 16 (B) from Paxinos and Watson (1998). Figure adapted from Paxinos and Watson (1998).

2.11. Cytochrome c immunohistochemistry

Immunohistochemistry for cyt c (1:100: rabbit anti-rat: Cell Signaling Technology) was performed. Sections were deparaffinized using 3 xylene immersions of 5 minutes each followed by 2 100% ethanol baths for 10 minutes and 2 90% ethanol baths for 10 minutes. Sections were then washed using distilled water followed by antigen unmasking with ready-to-use proteinase K (Dako). A solution containing 0.03% hydrogen peroxide in 50% methanol was then applied to the tissue in a humidifying chamber for 30 minutes to reduce the number of active endogenous peroxidases present prior to rinsing with distilled water and tris-buffered saline (TBS) containing 0.1% Triton X-100. Following hydrogen peroxide application, a blocker comprised of 10% normal horse serum (NHS) and TBS with 0.1% Triton X-100 was applied to reduce non-specific background staining.

The primary antibody (1%: cyt c) was added to a solution of 10% NHS and 89% TBS with Triton X-100 to the tissue and incubated overnight at a temperature of 4 ^{0}C. The following day, a secondary antibody (0.5%: whole rabbit immunoglobulins) was applied in a solution of 10% NHS in TBS with 0.1% Triton X-100. A tertiary was applied after the secondary and it consisted of an avidin-biotin complex (ABC: 1%: Vector Laboratories) in solution with TBS with 0.1% Triton X-100. Tissue was then washed 3 times for 10 minutes each time with TBS with 0.1% Triton X-100. The complex consisting of the primary antibody, secondary antibody, and tertiary ABC was visualized using a tablet of 3,3' diaminobenzedine tetrahydrochloride (DAB, Sigma) in a solution consisting of 0.96% distilled water, 0.03% hydrogen peroxide, and TBS. After visualization with DAB, tissue was again washed 3 times for 10

minutes each using TBS with 0.1% Triton X-100. After washing, sections were dehydrated by immersion in 70% ethanol for 2 minutes, 90% ethanol twice for 2 minutes, 100% ethanol twice for 2 minutes, followed by 2 immersions in xylene for 2 minutes each. Sections were then coverslipped using permount mounting media.

Due to the presence of high levels of endogenous cyt c in sham animals, samples of tissue were stained using cyt c blocking peptide (Cell Signaling) and metal enhanced DAB (Sigma) to show the specificity of primary antibody binding and ensure that antibody binding was confined only to the target antigen. Prior to addition of the primary antibody, blocking peptide consisting of 2% cyt c blocker (Cell Signaling), 10% NHS, and TBS with 0.1% Triton X-100 was added to the tissue.

2.12. Immunohistochemistry analysis of cytochrome c

Cell counts were performed at X200 magnification using between 1 and 5 visual fields of the cortex, striatum, hippocampus, hypothalamus, and thalamus in the right hemisphere ipsilateral to the carotid artery ligation (Figure 2-3). Fields were selected based on anatomy represented in Figure 29 from Paxinos and Watson (1998) and chosen such that the majority of each region was represented. Photomicrographs were taken from images collected from a digital camera connected to an Olympus BX60 light microscope. Photomicrographs were recorded using ImagePro Plus v. 4.5.0.29 software such that no two fields overlapped. Cell counts were performed by an unbiased observer (SH) blind to treatment groups.

2.13. TUNEL staining

Labeling with terminal deoxynucleotidyl transferase mediated biotin-dUTP nick-end-labelling (TUNEL) was performed using an *in Situ* Cell Death Detection Kit

from Roche Applied Science (Laval, QC). Paraffin wax was melted at approximately 60 ^{0}C followed by deparaffinization in xylene, dehydration in graded ethanol baths and rinsing with dd$H_2$0. Permeabilization solution (0.1% sodium citrate and 0.1% triton X-100) was then added to the tissue to enhance permeability. Following rinsing with phosphate-buffered saline (PBS), TUNEL reaction mixture was added and the tissue was incubated for 60 minutes at 37 ^{0}C in a humid, dark environment to allow the TUNEL reaction mixture containing terminal deoxynucleotidyl transferase to bind to 3' DNA strand breaks in the tissue effectively (Roche Applied Sciences, 2006). Afterwards, tissue was rinsed again using PBS before converter-POD (containing sheep antibody binding peroxidase) was applied to the tissue as a tertiary. Converter-POD was followed by metal-enhanced DAB (Sigma-Aldrich) to visualize cells for microscopy.

2.14. TUNEL analysis

TUNEL staining was quantified in 18 different brain regions from a coronal brain section approximately -2.30 mm from bregma (Paxinos and Watson, 1998: Figure 29). Photomicrographs were taken using ImagePro Plus v. 4.5.0.29 at X100. Photomicrograph regions are shown in Figure 2-4. The proportion of TUNEL coverage in each area exhibiting staining was recorded by a blind observer as being 0% or approximately 0-24%, 25-49%, 50-74%, 75-99%, or 100% covered with TUNEL-stained cells. Representative photomicrographs depicting different percentages of TUNEL coverage are shown in Figure 2-5.

Following quantification of all stained regions by a blind observer, fields consistently showing the highest number of TUNEL stained regions were analyzed to

determine the quantity of staining present. Areas analyzed included the somatosensory cortex, lateral dorsal thalamus, and dorsal caudate. The percentage of each region covered by TUNEL-expressing cells was calculated by measuring the size of the field and the area of the field covered by TUNEL-stained cells using NIH imageJ v.1.37p. Areas that were lost due to lesion or reorganization of the brain after injury were not measured. The percentage of TUNEL coverage was compared between groups by means of a one-way ANOVA with Tukey's post-hoc test.

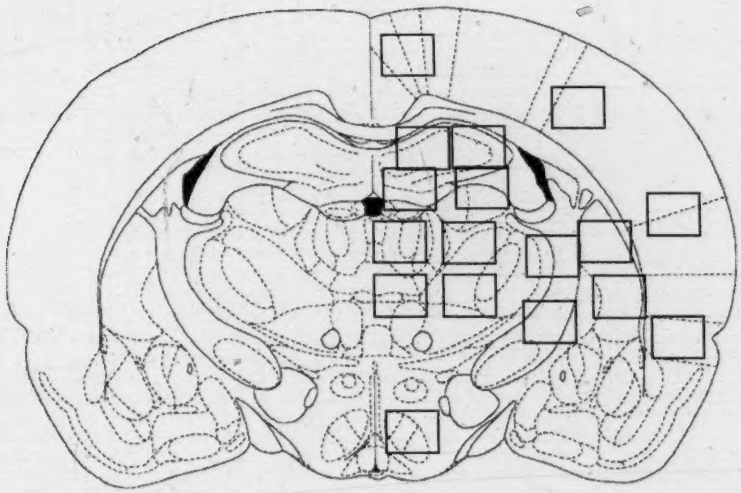

Figure 2-3. Cell count fields for cyt c immunohistochemistry analysis.

Cell count fields used for cyt c counts shown in ischemic hemisphere. Fields were photomicrographed at X200 magnificantion for analysis using ImagePro Plus v. 4.5.0.29. Figure adapted from Figure 29, Paxinos and Watson (1998).

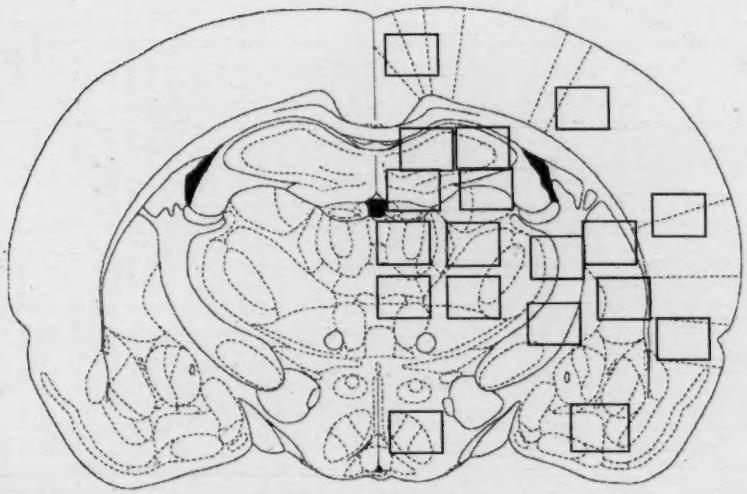

Figure 2-4. Regions selected for TUNEL analysis.

Fields selected for regional TUNEL staining analysis. Regions were identified using Paxinos and Watson (1998) to ensure that field overlap did not occur. Regional analysis was performed at X100 magnification. Diagram adapted from Figure 29, Paxinos and Watson (1998).

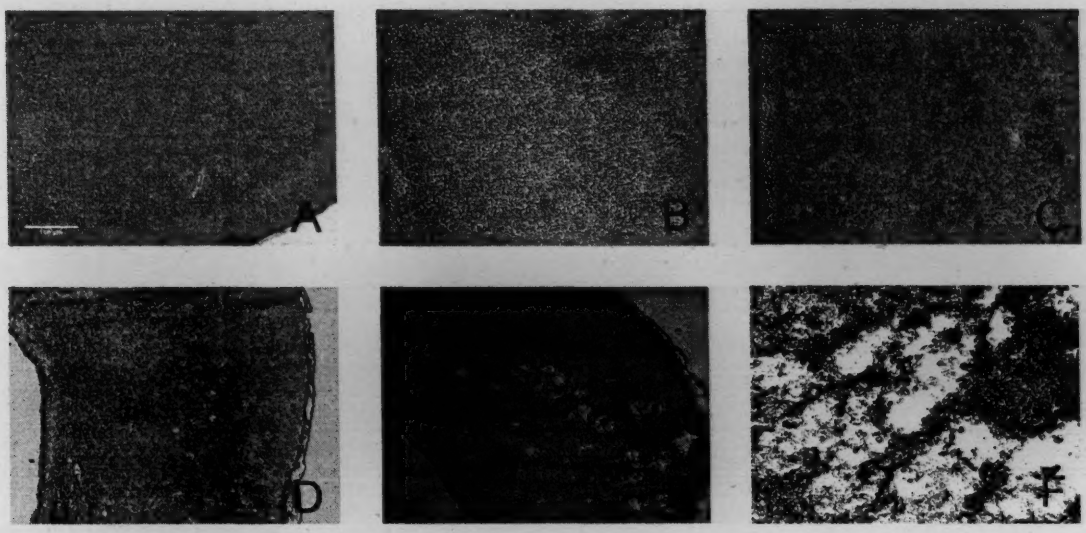

Figure 2-5. TUNEL field coverage.

Representative photomicrographs of TUNEL stained tissue. The scale bar in (A) represents 100 μm. Examples of different fields coverage by TUNEL stained cells. (A) shows a field with TUNEL coverage in the range of 0%. (B) demonstrates a field with less than 0-24% TUNEL cell coverage while (C) shows a range between 25-49% coverage. (D) and (E) show 50-74% and 74-99% coverage respectively while (F) shows an area with a lesion showing 100% TUNEL coverage of the remaining tissue.

CHAPTER 3: RESULTS

3.1. General observations

No noticeable differences in weight gain or appearance were observed between groups. Average mortality among all litters was 16.7% (30/180), similar to other studies using comparable methodology (Ohmura et al., 2005). Injections were tolerated at both low and high doses. Reflexes and suckling in the remaining animals were observed to function normally up to one week after HI.

3.2. Preliminary core temperature and blood glucose measurements

3.2.1. Core Temperature

Hypothermic animals did not display apnea or shivering in response to lowered core temperatures. Animals in the CH group had a mean core temperature of 28.91 ^{0}C during the 24-hour period in the while CN animals had a mean temperature of 36.13 ^{0}C. The mean temperature of the VH animals was 29.41 ^{0}C while VN animals had a mean temperature of 36.61 ^{0}C (Figure 3-1).

3.2.2. Blood glucose levels

Differences in blood glucose at 3.25% glucose in normothermic animals and 0.30% blood glucose in hypothermic animals were nonsignificant ($p>0.05$). Mean blood glucose in normothermic animals was found to be 4.99 mmol/L while blood glucose in hypothermic animals had a mean of 5.72 mmol/L (Figure 3-2).

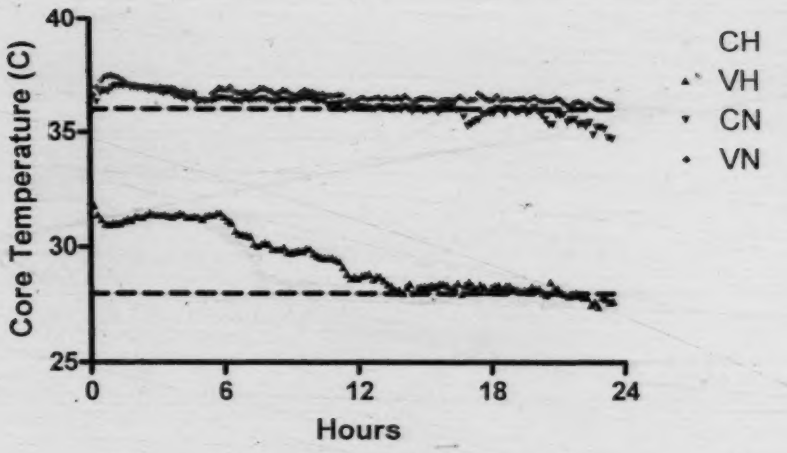

Figure 3-1. High-dose 24-hour core temperature measurements.

No differences in core temperatures were found between CH and VH groups or between CN and VN groups. Dotted lines represent baseline temperatures for hypothermic (28.5 °C + -0.5 °C) and normothermic (36.5 °C + -0.5 °C) baths respectively.

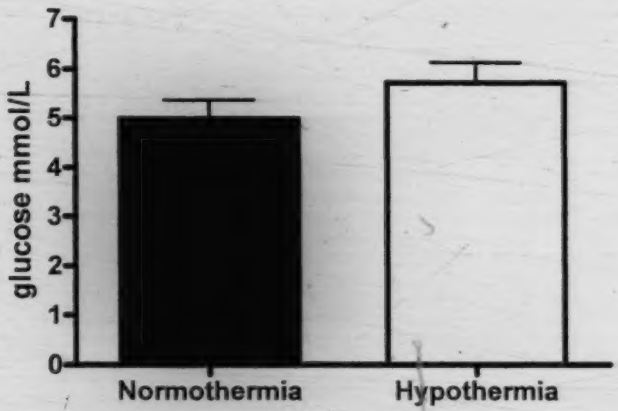

Figure 3-2. High-dose blood glucose measurements

No significant differences in blood glucose were seen between normothermic or hypothermic animals.

3.2.3. Damage.ranking

After half of the animals used in the 3 mg/kg study were sacrificed (45 animals), visual ranking of brain damage was performed. Ranking was performed again once all animals in the treatment groups (CH, CN, VH, and VN) had been sacrificed (a total of 90 animals). Once all brains in the 3 mg/kg study had been ranked, a one-way ANOVA showed no significant differences between groups (Figure 3-3). In the high-dose (3 g/kg) study, brains were ranked after all animals in the study had been sacrificed (150). A one-way ANOVA with Tukey's post-hoc test revealed differences between VN and VH animals ($p<0.05$), VN and CH animals ($p<0.001$), and CN and CH animals ($p<0.05$). Results are shown in Figure 3-4.

3.3. Infarct volume

In 3 mg/kg animals, a one-way ANOVA with Tukey's post-hoc test found no significant differences between groups (Figure 3-5). A one-way ANOVA with Tukey's post-hoc analysis showed that infarct volume was significantly reduced in CH animals compared to CN animals ($p<0.01$) and VN animals ($p<0.001$). VH animals also had smaller infarct volume compared to CN animals ($p<0.01$) and VN animals ($p<0.01$: Figure 3-6). Representative photomicrographs of high-dose infarct volume are shown in Figure 3-7.

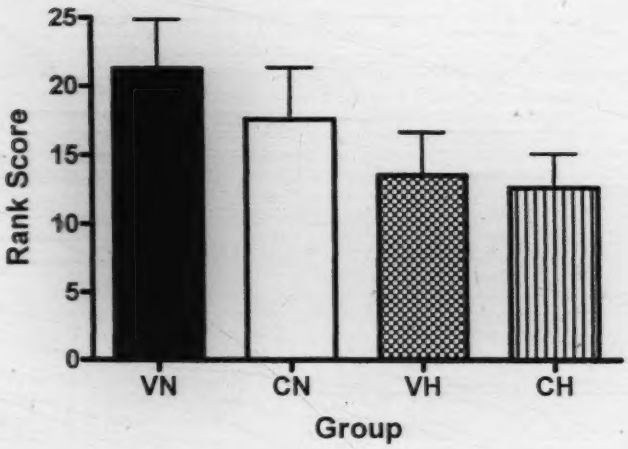

Figure 3-3. Low-dose damage ranking.

No statistically significant differences were seen between groups when visual ranking was used to examine low-dose treated brains.

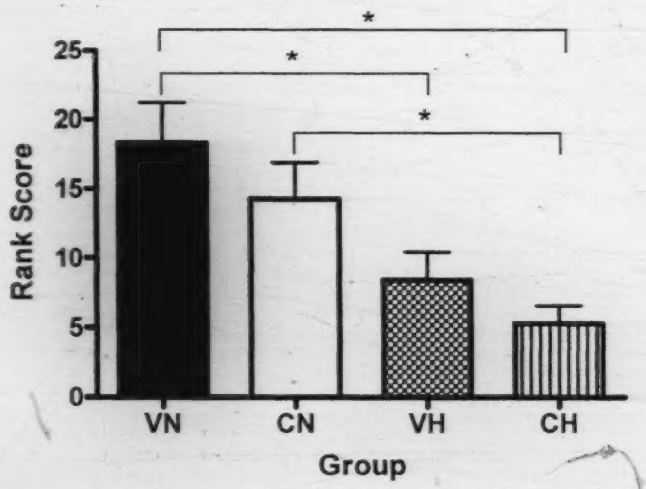

Figure 3-4. High-dose damage ranking.

The results of a one-way ANOVA with Tukey's post-hoc test of damage ranking performed on high-dose (3 g/kg) brains showed that CH animals had significantly less damage than CN animals ($P < 0.05$) and significantly less damage than VN animals ($p < 0.001$). VH animals showed less damage than VN animals ($p < 0.01$).

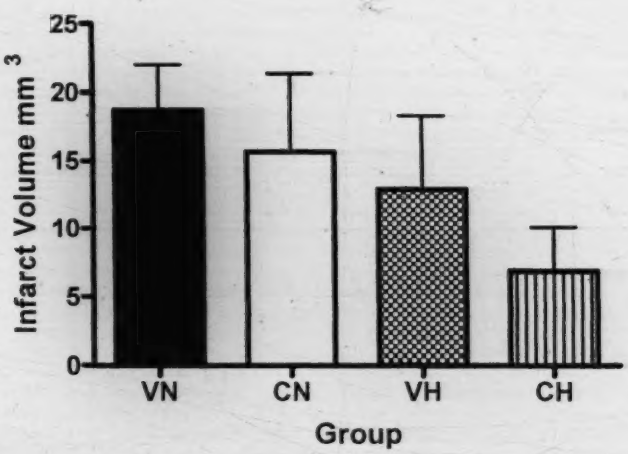

Figure 3-5. Low-dose infarct volume.

Animals in the 3 mg/kg study showed no statistically significant differences in infarct volume.

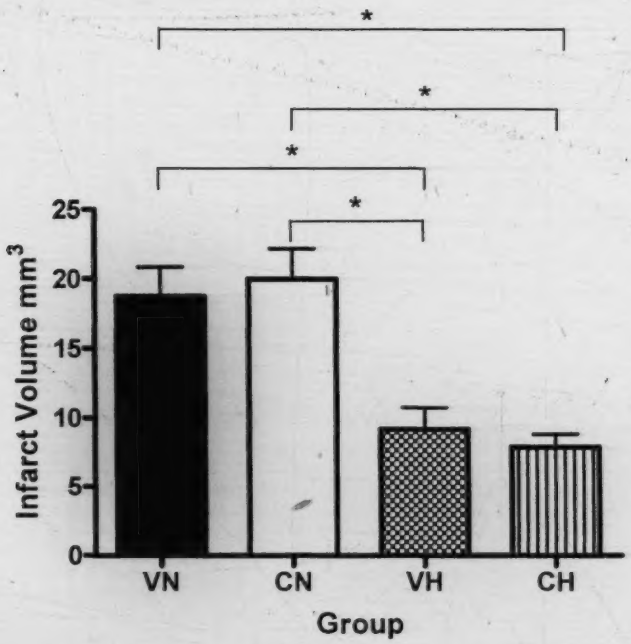

Figure 3-6. High-dose infarct volume.

Infarct volume was significantly reduced in CH animals compared to CN animals ($p < 0.01$) and VN animals ($p < 0.001$). As well, VH animals had reduced infarct volume compared to CN animals ($p < 0.01$) and VN animals ($p < 0.01$).

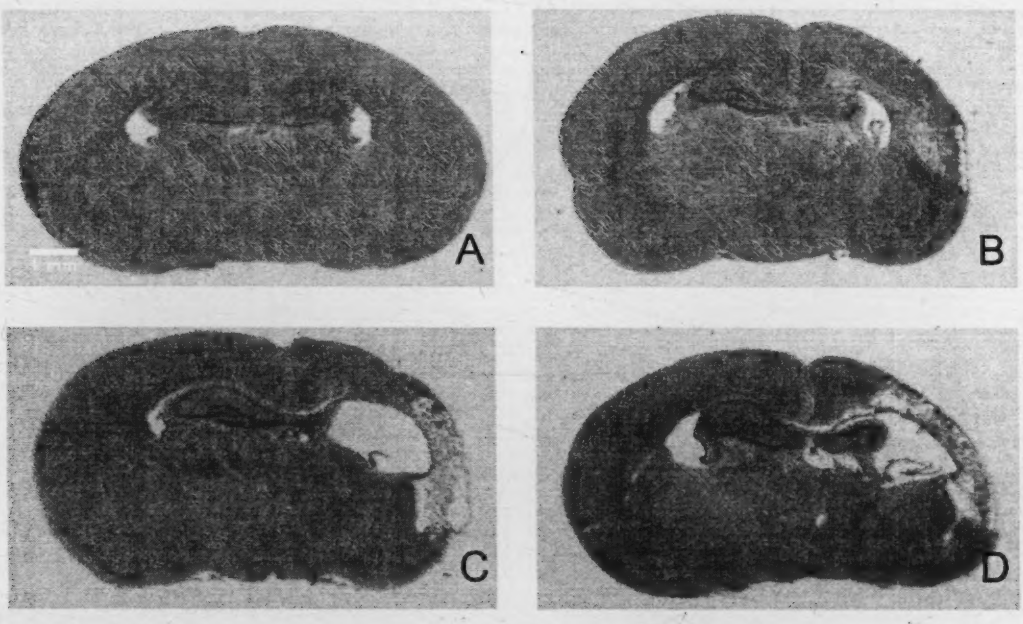

Figure 3-7. Infarct volume representative photomicrographs.

Representative photomicrographs of lesion size in CH (A), VH (B), VN (C), and CN (D) groups. Infarct size was measured using NIH imageJ v.1.37p. Scale bar in A equivalent to 1 mm.

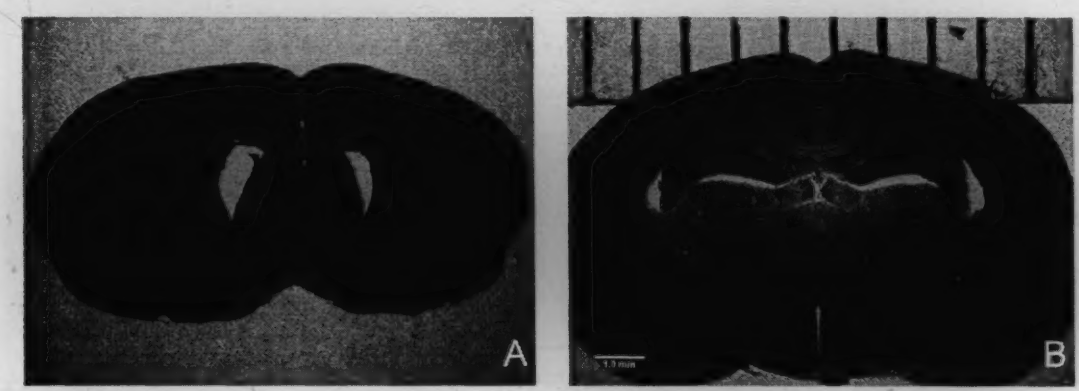

Figure 3-8. H and E staining for white matter thickness analysis.

Representative photomicrographs of H and E stained sections used to determine white matter thickness. Anterior sections are shown in A, while posterior sections are shown in B. Photomicrographs of posterior sections (B) were taken along with a scale set in mm. The scale bar in B represents 1 mm.

3.4. White matter damage

Representative photomicrographs of H and E stained sections used for external capsule thickness measurements are shown in Figure 3-8. An analysis of external capsule thickness showed that in anterior sections of the external capsule (Figure 3-9), CH animals had significantly greater external capsule thickness than CN animals ($p<0.01$) and VN treated animals ($p<0.001$). The posterior external capsule (Figure 3-10) of CH animals was significantly thicker than CN treated animals ($p<0.01$). CH animals also had significantly thicker external capsule than VN treated animals ($p<0.001$).

3.5. Cytochrome c cell counts

Representative photomicrographs of cyt c staining by group and the antigen blocking trial are shown in Figure 3-11. Cyt c cell counts showed no significant differences between groups. However, cell counts were consistently higher in all regions in CH and VH groups as opposed to CN and VN groups. The results of cyt c cell counts are shown in Figure 3-12.

3.6. TUNEL staining

Significant numbers of TUNEL labelled cells appeared only in the hemisphere ipsilateral to HI. Regions (as shown in Figure 2-5) demonstrating TUNEL staining were more common in VN and CN animals, with fewer TUNEL stained areas observed in CH and VH animals. A greater number of regions containing TUNEL labelled cells were observed in normothermic (CN and VN) groups. In contrast, regions demonstrating 0-24% and 25-49% expression were more commonly observed in hypothermic (CH and VH) groups (Figure 3-13). When the percentage of TUNEL

coverage was determined, a trend towards a group effect was demonstrated by a one-way ANOVA in both the lateral dorsal thalamus ($p = 0.0582$) and the somatosensory cortex ($p = 0.0605$). Results of the one-way ANOVA are shown in Figure 3-14.

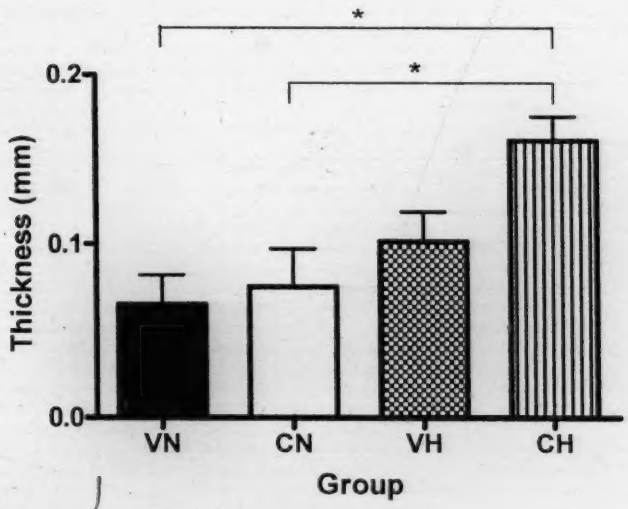

Figure 3-9. Analysis of anterior external capsule.

The anterior external capsule showed increased thickness in CH animals compared to the CN group ($p < 0.01$) and VN group ($p < 0.001$).

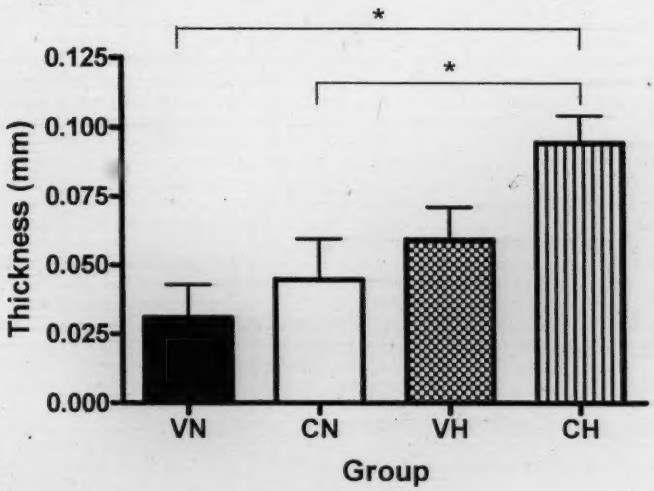

Figure 3-10. Analysis of posterior external capsule.

Histogram displaying posterior external capsule thickness in mm. Animals treated with CH had significantly thicker posterior external capsule than CN animals ($p < 0.05$) and VN animals ($p < 0.01$).

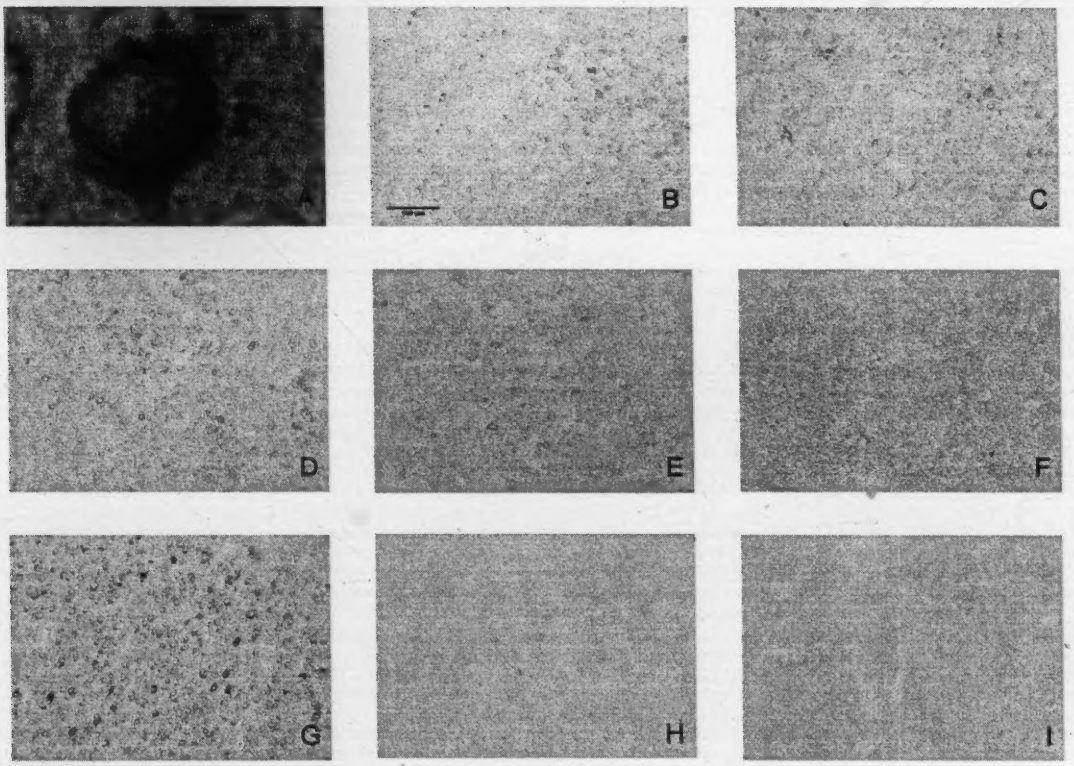

Figure 3-11. Cyt c immunohistochemistry photomicrographs.

High levels of cyt c immunoreactivity were seen in the cytoplasm, indicating release of cyt c through the MTP (A). (A) is a close-up view of a cyt c expressing cell at X400 magnification with imaging software enhancement. Sections from (B) CH, (C) VH, (D) CN, (E) VN, (F) HIC, and (G) sham treated animals are shown respectively. Representative photomicrographs are taken from coronal sections of the retrosplenial cortex. Results of the cyt c blocker study are shown in (H) for sham animals and (I) for negative control staining. Scale bar in (B) equivalent to 100 μm.

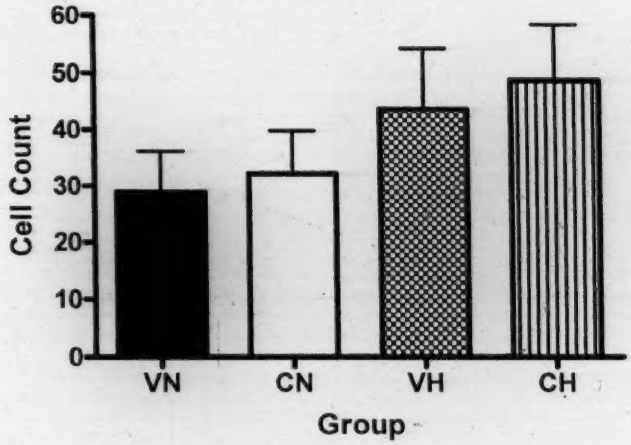

Figure 3-12. Cyt c immunohistochemistry cell counts.

Cell counts were consistently higher in CH and VH animals as opposed to CN and VN animals. However, no statistically significant differences between groups were seen.

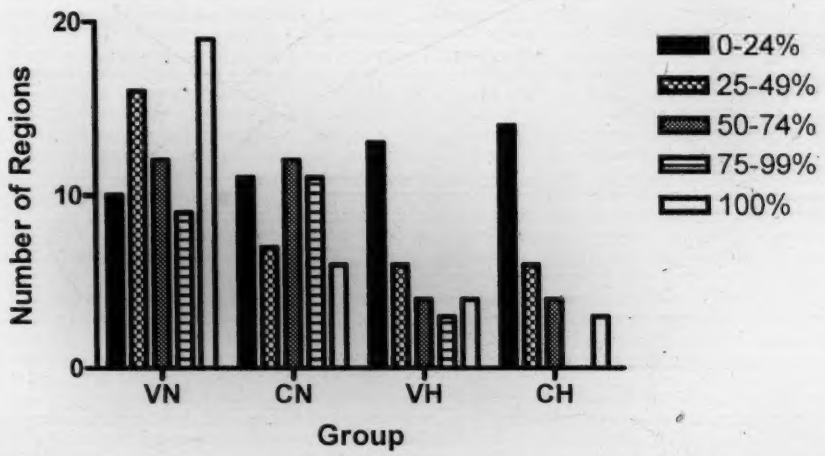

Figure 3-13. TUNEL-expressing brain regions.

More TUNEL-expressing regions were seen in VN and CN animals as opposed to VH and CH animals. Many more fields in the VN and CN animals displayed 100% and 75-99% coverage by TUNEL-expressing cells. In contrast, the majority of TUNEL-stained regions in VH and CH animals showed 0-24% or 25-49% coverage.

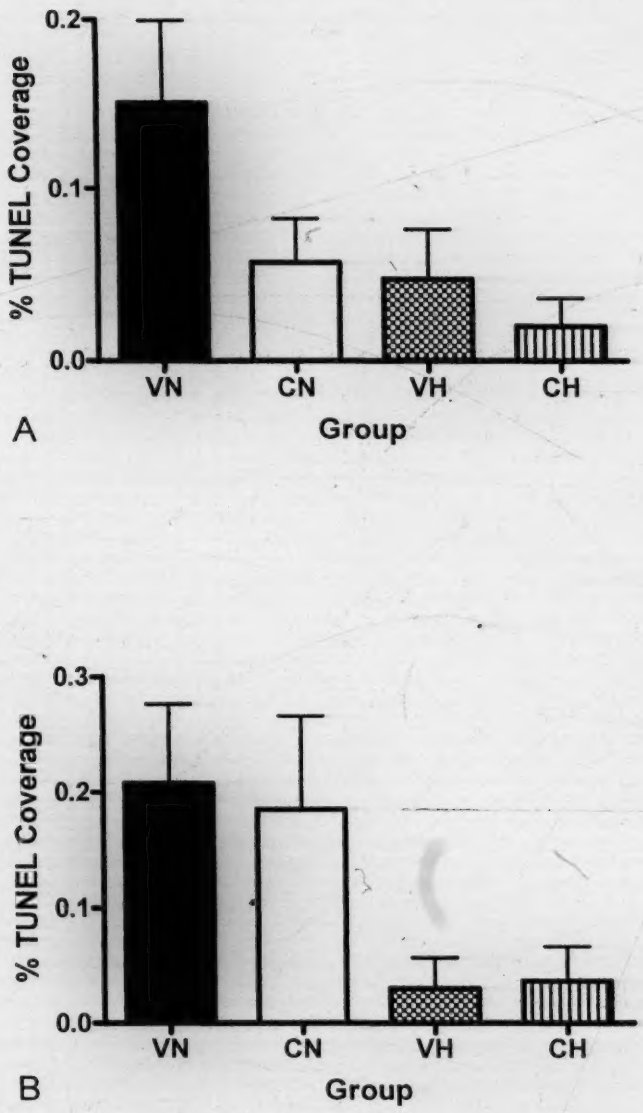

Figure 3-14. Percentage of TUNEL coverage in lateral dorsal thalamus (A) and somatosensory cortex (B) fields.

No significant differences in TUNEL coverage were observed between treatment groups. A trend towards significance was observed in the lateral dorsal thalamus (A: $p = 0.0582$). and somatosensory cortex (B: $p = 0.0605$) fields.

CHAPTER 4: DISCUSSION

4.1. Overview

In the current study, we determined whether Cr would be effective as a neuroprotective agent post-HI, alone and in combination with hypothermia. Preliminary data showed that core temperature and blood glucose were not significantly altered by administration of Cr. Findings also showed that CH and VH treatment significantly reduced infarct volume compared to VN or CN treatment. However, while Cr treated animals did show a decrease in damage on various treatment measures, the differences between Cr and vehicle groups were not statistically significant.

4.2. Neuroprotection in white matter

CH animals showed increased neuroprotection compared to VN and CN treated animals. These effects may be accounted for by the fact that white matter is vulnerable to HI due to the developmental stage of oligodendrocyte precursors (OPCs) present and the myelination processes that they orchestrate. By damaging OPCs early in development while they are in their proliferation stage, permanent deficiencies in myelination can emerge (Back et al., 2002). After HI, damaged OPCs myelinate fewer axons with radically altered connectivity in white matter tracts resulting (Calvert and Zhang, 2005). Despite severe damage being expected in white matter structures such as the external capsule, significantly greater external capsule thickness was observed in the CH group compared to the CN and VN groups.

The protective effect seen in the CH animals may have required the combined effects of both Cr and hypothermia together to prevent damage to OPCs during

development. For example, a factor that may have increased the neuroprotection seen in the external capsule is the greater utilization of Cr in white matter. High-dose oral Cr studies in humans have reported much greater increases in white matter total Cr (11.5%) than in grey matter (4.7%) or cerebellum (5.4%) and more Cr may be able to enter white matter to protect it from apoptosis (Persky and Brazeau, 2001). As well, CK mRNA has been found to be present in greater amounts in both astrocytes and oligodendrocytes as opposed to neurons, indicating that a greater availability of ATP and PCr may have been created in the white matter of CH animals (Molloy et al., 1992).

The combined effects of hypothermia could also increase the neuroprotective potency of Cr due to physiological changes following HI. For example, many drugs have been documented to have a longer half-life under hypothermic conditions (Thoresen and Whitelaw, 2003). Cr may be an example of such a drug, as Cr has been found to decay into creatinine more rapidly at low (acidic) pH and at higher temperatures (Wyss and Kaddurah-Daouk, 2000). As therapeutic hypothermia reduces brain temperature and aids in returning physiological pH to normal during reperfusion, hypothermia could prevent Cr break-down following injury and improve neuroprotection (Erecinska, Thoresen, and Silver, 2003).

4.3. Cytochrome c release and apoptosis

Despite being a indicator of apoptotic activity, cyt c expression was increased in CH and VH animals compared to CN and VN animals. Several explanations for this effect can be made based on the timing of pruning activity in the developing brain and the degree of recovery following injury that was observed. For example, the

increase in cyt c in the CH and VH groups could be due to recovery rather than cell death because more viable cells could have been present to undergo pruning following HI in CH and VH animals. Because of the rapid development of the mammalian CNS shortly after birth, a large number of cells that are differentiated into neurons are terminated by means of apoptosis prior to having any functional role in the organization of the brain (Kolb and Whishaw, 2003). As well, apoptotic processes initiated by HI could increase the number of cells already being lost from normal cell pruning in animals suffering less damage after HI such as the CH and VH groups (Blomgren, Leist, and Groc, 2007).

However, almost all cells die from the prolonged effects of an HI insult within 7 days in the rat model of HI (Gunn and Thoresen, 2006). Because the time of sacrifice in the current study was PND 14, many of the cells lost due to apoptosis would have been eliminated well before the time of sacrifice. Many of the cells showing signs of cyt c release would likely be dying due to developmental apoptosis as a result. In the case of animals in the CH and VH groups, the number of cells available by PND 14 was much greater due to increased survival provided by Cr and hypothermia treatments. As a result, many more cells in CH and VH animals may have been available to undergo apoptosis later on due to pruning and reorganization processes occurring in the brain, which the higher cyt c cell counts reflect.

4.4. TUNEL and apoptosis

Despite the increase in cyt c observed in CH and VH animals, TUNEL-stained cells were more common in VN and CN animals than in CH and VH animals, as represented by the larger number of regions expressing TUNEL stain. In contrast with

cyt c expression, TUNEL results may indicate that although many cells in the CH and VH groups were demonstrating cyt c release, more cells in the VN and CN groups had undergone DNA fragmentation and the final stages of apoptosis. The increased TUNEL staining in VN and CN animals in contrast to the increased cyt c release in VH and CH animals may also indicate that apoptotic cell death was being finalized in the VN and CN groups while apoptosis had been initiated in VH and CH animals.

The increase in TUNEL staining seen in the VN and CN groups may also have been the result of cells dying due to altered developmental apoptosis after HI. Evidence for developmental alterations in apoptosis can be seen from changes in the density of TUNEL staining across different brain regions. Regions in VN and CN groups showed greater TUNEL expression, including a much greater number of areas with 75-99% and 100% TUNEL expression, particularly in lesioned areas. In contrast, the majority of regions showing TUNEL staining in the VH and CH animals demonstrated 0-24% and 25-49% coverage.

As well, high rates of apoptosis may occur in areas where extensive necrotic cell loss has already occurred. For example, many of the areas showing 75-99% or 100% TUNEL coverage in VN and CN animals were adjacent to visible lesions during analysis. These findings may be explained by the fact that the brain extensively prunes cell populations and alters connections in response to injury and quickly removes cells that are no longer part of functional neural networks following ischemic injury (Kolb and Whishaw, 2003).

4.5. Creatine as a neuroprotective treatment

In the current study, Cr did not significantly enhance neuroprotection compared to vehicle alone or hypothermia alone. However, Cr likely did not fail to provide neuroprotection due to the injection volume, which was more than adequate to provide maximal effect based on other Cr research (Adcock et al., 2002; Holtzman et al., 1998; Berger et al., 2004). Publications that have shown increased PCr and ATP levels in a similar rat model to the one used in the current study can be used to speculate on the effects of the 3 g/kg dose used. For instance, Cr injected at 3 g/kg body weight has been shown to significantly increase the ratio of ATP to other metabolites in PND 8 rats (Adcock et al., 2002). A significant increase in Cr and ADP/AMP phosphorylation has also been noted in a similar rat model using a 3 g/kg dose of Cr (Holtzman et al., 1998).

In addition to evidence for 3 g/kg being an effective dose in *in vivo* models, *in vitro* work using Cr has shown that concentrations of Cr beyond 1 mM do not further enhance neuroprotection (Balestrino et al., 1999). These concentrations were surpassed in the current study as the concentration of Cr administered was very near the maximum solubility of Cr in saline solution at the time of injection. As a result, it is probable that Cr supplementation was adequate to provide or even surpass the neuroprotective dose used in various pre-HI studies.

Another conclusion that may be drawn based on the lack of improvement observed in the Cr groups compared to the vehicle groups is that the energy recovery provided by Cr may be inadequate to influence neuroprotection significantly. The slight but nonsignificant increase in neuroprotection seen in groups treated with Cr

may be taken as evidence of this possibility. The non-significant increase in neuroprotective measures observed may be the result of Cr's protective effects other than energy recovery, including ROS sequestration (Lawler et al., 2002).

A second possibility for the ineffectiveness of Cr observed in the current study is that Cr does not cross the BBB quickly enough to provide improved neuroprotection. In hypothermia studies, it has been found that administering hypothermia as soon as possible following injury maximizes neuroprotection (Gunn and Thoresen, 2006; Alzaga, Cerdan, and Varon, 2006). Since energy recovery is hypothesized to be the main mechanism of neuroprotection for both Cr and hypothermia, increasing energy recovery as rapidly as possible after HI produces better neuroprotection as neuroprotection is increased when hypothermia is applied as soon as possible after HI (Perlman, 2006). If Cr were to cross the BBB too slowly to be neuroprotective, it might suffer from the same problems faced by late administration of hypothermia and be less effective as a result.

Studies that have shown Cr at 3 g/kg to be successful in treating HI injury have given Cr prior to HI, not after HI as in the current study (Adcock et al., 2002; Holtzman et al., 1998; Berger et al., 2004), avoiding the problem of treatment timing during the recovery phase. However, Cr given following HI was not significantly neuroprotective in the current study. As a result, it may be possible that Cr does not enter brain parenchyma quickly enough to provide neuroprotection following HI, although it can build up in a rat pup to provide protection by PND 7 when injections begin several days earlier.

Another possibility other than delay of Cr perfusion following injection is that energy recovery is not the primary mechanism by which neuroprotection is derived. In the literature, SEF has been described as a byproduct of secondary cell death processes rather than a cause of cell death in the post-HI period. According to the byproduct theory of SEF, hypothermia is effective not due to its ability to increase energy recovery after HI but because of its influence on other pathological mechanisms that prevent cell death from occurring (Vannucci, Towfighi, and Vannucci, 2004). If the byproduct theory is true, Cr should not be effective and energy recovery is not related to recovery. Future studies will be necessary to further elucidate post-HI energy recovery and outcome.

4.6. Future studies

4.6.1. Use of creatine in adults

Due to the fact that CK is more prevalent in older animals and adults (Holtzman et al., 1993), that Cr is used commonly as an energy supplement in humans (Wyss and Kaddurah-Daouk, 2000), and in light of Cr's success as a pre-ischemic treatment, it might be efficacious to administer Cr as a supplement to adults who are at risk of stroke. For example, Prass et al. (2007) have shown that oral Cr supplementation reduces infarct size in an *in vivo* mouse model of adult stroke. Future studies could model adult stroke and provide Cr alone prior to ischemia along with hypothermia to provide improved neuroprotection.

4.6.2. Creatine supplementation to unborn fetuses

As well as being effective in adults, many studies have shown that Cr is effective at providing neuroprotection prior to HI. Despite the obvious drawback of

pre-HI Cr supplementation, it may be possible to infuse Cr to the unborn fetus through the mother to provide prophylactic protection from HI during birth (Adcock et al., 2002). In rat studies from the 1970s utilizing radioactively labelled Cr, transport of Cr across the placenta into the fetus has been noted and Cr has been found to actively cross the placental barrier and accumulate in the fetus through the placental unit (Koszalka, Jensh, and Brent, 1975). The proposed mechanism for Cr build-up is diffusion down Cr's concentration gradient, leading to an increase of Cr levels in the infant (Davis et al., 1978). Despite these promising findings in rat models, little work has been done since the 1970s and no human research addressing Cr's ability to cross the placental barrier appears in the literature.

4.6.3. Alternative combination mechanisms

Although the combination treatment chosen in the current study was not shown to be successful, combination treatments focusing on mechanisms further downstream in the injury process may be more successful. For example, hypothermia has been noted to reduce many damaging mechanisms of inflammation. These include harmful microglia activation, neutrophil penetration (Inamasu et al., 2000), the expression of endothelial adhesion molecules, leukocyte penetration (Wang et al., 2002), and the reduced expression of proinflammatory cytokines such as TNF-α (Yenari and Han, 2006).

Combination drugs that suppress inflammation could be given alongside hypothermia to further increase inflammatory inhibition and enhance neuroprotection. For example, doxycycline has been successful when given post-HI in neonatal rat models and may provide a good candidate co-treatment for hypothermia (Jantzie et al.,

2005). As a result, doxycycline may be able to provide increased neuroprotection when combined with hypothermia. The anti-inflammatory drug dipyrone has already been investigated in a combination therapy study where dipyrone and hypothermia together were seen to reduce neuronal damage by 50% (Coimbra et al., 1996).

Alternatively, many different mechanisms could be utilized to maximize protection of brain tissue after HI. A variety of pharmaceutical agents could be administered at the same time, providing cross-talk between the different drugs and side effects would be benign for a particular cocktail of treatments. A combination of agents could provide comprehensive treatment acting on a variety of mechanisms including excitotoxic glutamate release, ROS generation, and the inflammatory response simultaneously.

4.7. Conclusions

The experiments in the current thesis represent the first study to investigate combined Cr and hypothermia as co-treatments to improve neuroprotection following neonatal HI in a rat model. However, Cr does not increase neuroprotection significantly when compared to hypothermia or vehicle alone. Since enhancing energy recovery has been theorized to be one of the primary neuroprotective mechanisms of Cr, energy recovery may not be as important a mechanism of cell death as previously thought. SEF has been described as a byproduct of cell death (Vannucci, Towfighi, and Vannucci, 2004), and the current data would agree with such an interpretation.

REFERENCES

Adcock KH, Nedelcu J, Loenneker T, Martin E, Wallimann T, Wagner BP. Neuroprotection of creatine supplementation in neonatal rats with transient cerebral hypoxia-ischemia. Dev Neurosci. 2002;24(5):382-8.

Alkan T, Kahveci N, Buyukuysal L, Korfali E, Ozluk K. Neuroprotective effects of MK- 801 and hypothermia used alone and in combination in hypoxic-ischemic brain injury in neonatal rats. Arch Physiol Biochem 2001 Apr;109(2):135-44.

Alzaga AG, Cerdan M, Varon J. Therapeutic hypothermia. Resuscitation 2006 Sep;70(3):369-80.

Andersohn F, Konzen C, Garbe E. Systematic review: agranulocytosis induced by nonchemotherapy drugs. Ann Intern Med 2007 May;146(9):657-65.

Arpino C, D'Argenzio L, Ticconi C, Di Paolo A, Stellin V, Lopez L, Curatolo P. Brain damage in preterm infants: etiological pathways. Ann Ist Super Sanita 2005;41(2):229-37.

Asai S, Zhao H, Kohno T, Takahashi Y, Nagata T, Ishikawa K. Quantitative evaluation of extracellular glutamate concentration in postischemic glutamate re-uptake, dependent on brain temperature, in the rat following severe global brain ischemia. Brain Res 2000 May;864(1):60-8.

Back SA, Han BH, Luo NL, Chricton CA, Xanthoudakis S, Tam J, Arvin KL, Holtzman DM. Selective vulnerability of late oligodendrocyte progenitors to hypoxia-ischemia. J Neurosci 2002 Jan;22(2):455-63.

Badr Zahr LK, Purdy I. Brain injury in the infant: the old, the new, and the uncertain. J Perinat Neonatal Nurs 2006 Apr-Jun;20(2):163-75.

Balestrino M, Lensman M, Parodi M, Perasso L, Rebaudo R, Melani R, Polenov S, Cupello A. Role of creatine and phosphocreatine in neuronal protection from anoxic and ischemic damage. Amino Acids 2002;23(1-3):221-9.

Balestrino M, Rebaudo R, Lunardi G. Exogenous creatine delays anoxic depolarization and protects from hypoxic damage: dose-effect relationship. Brain Res 1999 Jan;816(1):124-30.

Banasiak KJ, Xia Y, Haddad GG. Mechanisms underlying hypoxia-induced neuronal apoptosis. Prog Neurobiol 2000 Oct;62(3):215-49.

Berger C, Schabitz WR, Wolf M, Mueller H, Sommer C, Schwab S. Hypothermia and brain-derived neurotrophic factor reduce glutamate synergistically in acute stroke. Exp Neurol 2004 Feb;185(2):305-12.

Berger R, Garnier Y. Pathophysiology of perinatal brain damage. Brain Res Brain Res Rev 1999 Aug;30(2):107-34.

Berger R, Middelanis J, Vaihinger HM, Mies G, Wilken B, Jensen A. Creatine protects the immature brain from hypoxic-ischemic injury. J Soc Gynecol Investig 2004 Jan;11(1):9-15.

Bernardi P, Krauskopf A, Basso E, Petronilli V, Blachy-Dyson E, Di Lisa F, Forte MA. The mitochondrial permeability transition from in vitro artifact to disease target. FEBS J 2006 May;273(10):2077-99.

Bona E, Hagberg H, Loberg EM, Bagenholm R, Thoresen M. Protective effects of moderate hypothermia after neonatal hypoxia-ischemia: short- and long- term outcome. Pediatr Res 1998 Jun;43(6):738-45.

Björkman ST, Foster KA, O'driscoll SM, Healy GN, Lingwood BE, Burke C, Colditz PB. Hypoxic/Ischemic models in newborn piglet: comparison of constant FiO2 versus variable FiO2 delivery. Brain Res 2006 Jul;1100(1):110-7.

Blomgren K, Leist M, Groc L. Pathological apoptosis in the developing brain. Apoptosis 2007 May;12(5):993-1010.

Blomgren K, Zhu C, Hallin U, Hagberg H. Mitochondria and ischemic reperfusion damage in the adult and in the developing brain. Biochem Biophys Res Commun 2003 May;304(3):551-9.

Bohnhorst B, Geuting T, Peter CS, Dordelmann M, Wilken B, Poets CF. Randomized, controlled trial of oral creatine supplementation (not effective) for apnea of prematurity. Pediatrics 2004 Apr;113(4):303-307.

Brewer GJ, Wallimann TW. Protective effect of the energy precursor creatine against toxicity of glutamate and beta-amyloid in rat hippocampal neurons. J Neurochem 2000 May;74(5):1968-78.

Brustovetsky N, Brustovetsky T, Dubinsky JM. On the mechanisms of neuroprotection by creatine and phosphocreatine. J Neurochem 2001 Jan;76(2):425-34.

Calvert JW, Zhang JH. Pathophysiology of an hypoxic-ischemic insult during the perinatal period. Neurol Res 2005 Apr;27(3):246-60.

Camacho A, Massieu L. Role of glutamate transporters in the clearance and release of glutamate during ischemia and its relation to neuronal death. Arch Med Res 2006 Jan;37(1):11-8.

Chang HY, Yang X. Proteases for cell suicide: functions and regulation of caspases. Microbiol Mol Biol Rev 2000 Dec;64(4):821-46.

Chowdhury I, Tharakan B, Bhat GK. Current concepts in apoptosis: the physiological suicide program revisited. Cell Mol Biol Lett 2006;11(4):506-25.

Clarkson AN, Sutherland BA, Appleton I. The biology and pathology of hypoxia-ischemia: an update. Arch Immunol Ther Exp (Warsz) 2005 May;53(3):213-25.

Coimbra C, Drake M, Boris-Moller F, Wieloch T. Long-lasting neuroprotective effect of postischemic hypothermia and treatment with an anti-inflammatory/antipyretic drug. Evidence for chronic encephalopathic processes following ischemia. Stroke 1996 Sep;27(9):1578-85.

Comi AM, Weisz CJ, Highet BH, Johnston MV, Wilson MA. A new model of stroke and ischemic seizures in the immature mouse. Pediatr Neurol 2004 Oct;31(4):254-7.

Davis BM, Miller RK, Brent RL, Koszalka TR. Materno-fetal transport of creatine in the rat. Biol Neonate 1978;33(1-2):43-54.

Delivoria-Papadopoulos M, Mishra OP. Mechanisms of perinatal cerebral injury in fetus and newborn. Ann N Y Acad Sci 2000;900:159-68.

Deng H, Han HS, Cheng D, Sun GH, Yenari MA. Mild hypothermia inhibits inflammation after experimental stroke and brain inflammation. Stroke 2003 Oct;34(10):2495-501.

Dirnagl U, Iadecola C, Moskowitz MA. Pathobiology of ischaemic stroke: an integrated view. Trends Neurosci 1999 Sep;22(9):391-7.

Edwards AD, Yue X, Squier MV, Thoresen M, Cady EB, Penrice J, Cooper CE, Wyatt JS, Reynolds EO, Mehmet H. Specific inhibition of apoptosis after cerebral hypoxia-ischaemia by moderate post-insult hypothermia. Biochem Biophys Res Commun 1995 Dec;217(3):1193-9.

Erecinska M, Thoresen M, Silver IA. Effects of hypothermia on energy metabolism in Mammalian central nervous system. J Cereb Blood Flow Metab 2003 May;23(5):513-30.

Estaquier J, Arnoult D. Inhibiting Drp1-mediated mitochondrial fission selectively prevents the release of cytochrome c during apoptosis. Cell Death Differ 2007 Jun;14(6):1086-94.

Giffard RG, Swanson RA. Ischemia-induced programmed cell death in astrocytes. Glia 2005 Jun;50(4):299-306.

Gluckman PD, Wyatt JS, Azzopardi D, Ballard R, Edwards AD, Ferriero DM, Polin RA, Robertson CM, Thoresen M, Whitelaw A, Gunn AJ. Selective head cooling with mild systemic hypothermia after neonatal encephalopathy: multicentre randomised trial. Lancet 2005 Feb;365(9460):663-70.

Golstein P, Kroemer G. Cell death by necrosis: towards a molecular definition. Trends Biochem Sci 2007 Jan;32(1):37-43.

Guan J, Bennet L, Gluckman PD, Gunn AJ. Insulin-like growth factor-1 and post-ischemic brain injury. Prog Neurobiol 2003 Aug;70(6):443-62.

Gunn AJ, Thoresen M. Hypothermic neuroprotection. NeuroRx 2006 Apr;3(2):154-69.

Hammer MD, Krieger DW. Hypothermia for acute ischemic stroke: not just another neuroprotectant. Neurologist 2003 Nov;9(6):280-9.

Harper N, Hughes M, MacFarlane M, Cohen GM. Fas-associated death domain protein and caspase-8 are not recruited to the tumor necrosis factor receptor 1 signaling complex during tumor necrosis factor-induced apoptosis. J Biol Chem 2003 Jul;278(28):25534-41.

Hashimoto T, Yonetani M, Nakamura H. Selective brain hypothermia protects against hypoxic-ischemic injury in newborn rats by reducing hydroxyl radical production. Kobe J Med Sci 2003;49(3-4):83-91.

Hazell AS. Excitotoxic mechanisms in stroke: an update of concepts and treatment strategies. Neurochem Int 2007 Jun;50(7-8):941-53.

Holtzman D, Togliatti A, Khait I, Jensen F. Creatine increases survival and suppresses seizures in the hypoxic immature rat. Pediatr Res 1998 Sep;44(3):410-4.

Holtzman D, Tsuji M, Wallimann T, Hemmer W. Functional maturation of creatine kinase in rat brain. Dev Neurosci 1993;15(3-5):261-70.

Hu X, Qiu J, Grafe MR, Rea HC, Rassin DK, Perez-Polo JR. Bcl-2 family members make different contributions to cell death in hypoxia and/or hyperoxia in rat cerebral cortex. Int J Dev Neurosci 2003 Nov;21(7):371-7.

Huerta S, Goulet EJ, Huerta-Yepez S, Livingston EH. Screening and detection of apoptosis. J Surg Res 2007 May;139(1):143-56.

Ide T, Tsutsui H, Kinugawa S, Utsumi H, Kang D, Hattori N, Uchida K, Arimura K, Egashira K, Takeshita A. Mitochondrial electron transport complex I is a potential source of oxygen free radicals in the failing myocardium. Circ Res 1999 Aug;85(4):357-63.

Ikonomidou C, Turski L. Why did NMDA receptor antagonists fail clinical trials for stroke and traumatic brain injury? Lancet Neurol 2002 Oct;1(6):383-6.

Inamasu J, Suga S, Sato S, Horiguchi T, Akaji K, Mayanagi K, Kawase T. Post-ischemic hypothermia delayed neutrophil accumulation and microglial activation following transient focal ischemia in rats. J Neuroimmunol 2000 Sep;109(2):66-74.

Jantzie LL, Cheung PY, Todd KG. Doxycycline reduces cleaved caspase-3 and microglial activation in an animal model of neonatal hypoxia-ischemia. J Cereb Blood Flow Metab 2005 Mar;25(3):314-24.

Jatana M, Singh I, Singh AK, Jenkins D. Combination of systemic hypothermia and N-acetylcysteine attenuates hypoxic-ischemic brain injury in neonatal rats. Pediatr Res 2006 May;59(5):684-9.

Jensen A, Garnier Y, Middelanis J, Berger R. Perinatal brain damage--from pathophysiology to prevention. Eur J Obstet Gynecol Reprod Biol 2003 Sep;110 Suppl 1:S70-S79.

Kimura T, Sako K, Tanaka K, Kusakabe M, Tanaka T, Nakada T. Effect of mild hypothermia on energy state recovery following transient forebrain ischemia in the gerbil. Exp Brain Res 2002 Jul;145(1):83-90.

Klivenyi P, Calingasan NY, Starkov A, Stavrovskaya IG, Kristal BS, Yang L, Wieringa B, Beal MF. Neuroprotective mechanisms of creatine occur in the absence of mitochondrial creatine kinase. Neurobiol Dis 2004 Apr;15(3):610-7.

Kolb B, Whishaw I. 2003. Human neuropsychology (5th ed). New York: Worth Publishers

Koszalka TR, Jensh RP, Brent RL. Placental transport of creating in the rat. Proc Soc Exp Biol Med 1975 Mar;148(3):864-9.

Lai AY, Todd KG. Hypoxia-activated microglial mediators of neuronal survival are differentially regulated by tetracyclines. Glia 2006 Jun;53(8):809-16.

Lawler JM, Barnes WS, Wu G, Song W, Demaree S. Direct antioxidant properties of creatine. Biochem Biophys Res Commun 2002 Jan;290(1):47-52.

Levine S. Anoxic-ischemic encephalopathy in rats. Am J Pathol 1960 Jan;36:1-17.

Li JM, Shah AM. ROS generation by nonphagocytic NADPH oxidase: potential relevance in diabetic nephropathy. J Am Soc Nephrol 2003 Aug;14(8 Suppl 3):S221-S226.

Ma D, Hossain M, Chow A, Arshad M, Battson RM, Sanders RD, Mehmet H, Edwards AD, Franks NP, Maze M. Xenon and hypothermia combine to provide neuroprotection from neonatal asphyxia. Ann Neurol 2005 Aug;58(2):182-93.

Ma D, Yang H, Lynch J, Franks NP, Maze M, Grocott HP. Xenon attenuates cardiopulmonary bypass-induced neurologic and neurocognitive dysfunction in the rat. Anesthesiology 2003 Mar;98(3):690-8.

Manos P, Bryan GK. Cellular and subcellular compartmentation of creatine kinase in brain. Dev Neurosci 1993;15(3-5):271-9.

Martinou JC, Youle RJ. Which came first, the cytochrome c release or the mitochondrial fission? Cell Death and Diff 2006 Jun;(13):1291-1295.

McDonald JW, Althomsons SP, Hyrc KL, Choi DW, Goldberg MP. Oligodendrocytes from forebrain are highly vulnerable to AMPA/kainate receptor-mediated excitotoxicity. Nat Med 1998 Mar;4(3):291-7.

Meyer LE, Machado LB, Santiago AP, da Silva WS, De Felice FG, Holub O, Oliveira MF, Galina A. Mitochondrial creatine kinase activity prevents reactive oxygen species generation: antioxidant role of mitochondrial kinase-dependent ADP re-cycling activity. J Biol Chem 2006 Dec;281(49):37361-71.

Molloy GR, Wilson CD, Benfield P, de Vellis J, Kumar S. Rat brain creatine kinase messenger RNA levels are high in primary cultures of brain astrocytes and oligodendrocytes and low in neurons. J Neurochem 1992 Nov;59(5):1925-32.

Moro MA, Almeida A, Bolanos JP, Lizasoain I. Mitochondrial respiratory chain and free radical generation in stroke. Free Radic Biol Med 2005 Nov;39(10):1291-304.

Munoz-Pinedo C, Guio-Carrion A, Goldstein JC, Fitzgerald P, Newmeyer DD, Green DR. Different mitochondrial intermembrane space proteins are released during apoptosis in a manner that is coordinately initiated but can vary in duration. Proc Natl Acad Sci U S A 2006 Aug;103(31):11573-8.

Northington FJ, Graham EM, Martin LJ. Apoptosis in perinatal hypoxic-ischemic brain injury: how important is it and should it be inhibited? Brain Res Brain Res Rev 2005 Dec;50(2):244-57.

O'Brien FE, Iwata O, Thornton JS, De Vita E, Sellwood MW, Iwata S, Sakata YS, Charman S, Ordidge R, Cady EB, Wyatt JS, Robertson NJ. Delayed whole-body cooling to 33 or 35 degrees C and the development of impaired energy generation consequential to transient cerebral hypoxia-ischemia in the newborn piglet. Pediatrics 2006 May;117(5):1549-59.

Ohmura A, Nakajima W, Ishida A, Yasuoka N, Kawamura M, Miura S, Takada G. Prolonged hypothermia protects neonatal rat brain against hypoxic-ischemia by reducing both apoptosis and necrosis. Brain Dev 2005 Oct;27(7):517-26.

Ohtsuki S, Tachikawa M, Takanaga H, Shimizu H, Watanabe M, Hosoya K, Terasaki T. The blood-brain barrier creatine transporter is a major pathway for supplying creatine to the brain. J Cereb Blood Flow Metab 2002 Nov;22(11):1327-35.

Ohtsuki S. Physiological function of blood-brain barrier transporters as the CNS supporting and protecting system. Yakugaku Zasshi 2004 Nov;124(11):791-802.

Paxinos G, Watson C. 1998. The rat brain in stereotaxic coordinates (4th ed). Toronto: Academic Press.

Perlman JM. Intervention strategies for neonatal hypoxic-ischemic cerebral injury. Clin Ther 2006 Sep;28(9):1353-65.

Persky AM, Brazeau GA. Clinical pharmacology of the dietary supplement creatine monohydrate. Pharmacol Rev 2001 Jun;53(2):161-76.

Prass K, Royl G, Lindauer U, Freyer D, Megow D, Dirnagl U, Stockler-Ipsiroglu G, Wallimann T, Priller J. Improved reperfusion and neuroprotection by creatine in a mouse model of stroke. J Cereb Blood Flow Metab 2006 Jun.

Ramani R. Hypothermia for brain protection and resuscitation. Curr Opin Anaesthesiol 2006 Oct;19(5):487-91.

Ravagnan L, Roumier T, Kroemer G. Mitochondria, the killer organelles and their weapons. J Cell Physiol 2002 Aug;192(2):131-37.

Rice JE, Vannucci RC, Brierley JB. The influence of immaturity on hypoxic-ischemic brain damage in the rat. Ann Neurol 1981 Feb;9(2):131-41.

Roche Applied Sciences. In Situ cell death detection kit, POD instruction manual (April, 2006). Accessed on November 26, 2007 from www.roche-applied-science.com

Roth SC, Baudin J, Cady E, Johal K, Townsend JP, Wyatt JS, Reynolds EO, Stewart AL. Relation of deranged neonatal cerebral oxidative metabolism with neurodevelopmental outcome and head circumference at 4 years. Dev Med Child Neurol 1997 Nov;39(11):718-25.

Sestili P, Martinelli C, Bravi G, Piccoli G, Curci R, Battistelli M, Falcieri E, Agostini D, Gioacchini AM, Stocchi V. Creatine supplementation affords cytoprotection in oxidatively injured cultured mammalian cells via direct antioxidant activity. Free Radic Biol Med 2006 Mar;40(5):837-49.

Shankaran S, Laptook A, Wright LL, Ehrenkranz RA, Donovan EF, Fanaroff AA, Stark AR, Tyson JE, Poole K, Carlo WA, Lemons JA, Oh W, Stoll BJ, Papile LA, Bauer CR, Stevenson DK, Korones SB, McDonald S. Whole-body hypothermia for neonatal encephalopathy: animal observations as a basis for a randomized, controlled pilot study in term infants. Pediatrics 2002 Aug;110(2 Pt 1):377-85.

Tanaka S, Takehashi M, Iida S, Kitajima T, Kamanaka Y, Stedeford T, Banasik M, Ueda K. Mitochondrial impairment induced by poly(ADP-ribose) polymerase-1 activation in cortical neurons after oxygen and glucose deprivation. J Neurochem 2005 Oct;95(1):179-90.

Tejkalova H, Kaiser M, Klaschka J, Stastny F. Does neonatal brain ischemia induce schizophrenia-like behaviour in young adult rats? Physiol Res 2006 Nov. Epublished.

Thoresen M, Whitelaw A. Therapeutic hypothermia for hypoxic-ischaemic encephalopathy in the newborn infant. Curr Opin Neurol 2005 Apr;18(2):111-6.

Toft PB. Prenatal and perinatal striatal injury: a hypothetical cause of attention-deficit-hyperactivity disorder? Pediatr Neurol 1999 Sep;21(3):602-10.

Toga AW, Thompson PM, Sowell ER. Mapping brain maturation. Trends Neurosci 2006 Mar;29(3):148-59.

Vannucci RC, Connor JR, Mauger DT, Palmer C, Smith MB, Towfighi J, Vannucci SJ. Rat model of perinatal hypoxic-ischemic brain damage. J Neurosci Res 1999 Jan;55(2):158-63.

Vannucci RC, Perlman JM. Interventions for perinatal hypoxic-ischemic encephalopathy. Pediatrics 1997 Dec;100(6):1004-14.

Vannucci RC, Towfighi J, Vannucci SJ. Secondary energy failure after cerebral hypoxia-ischemia in the immature rat. J Cereb Blood Flow Metab 2004 Oct;24(10):1090-7.

Vannucci RC, Vannucci SJ. Perinatal hypoxic-ischemic brain damage: evolution of an animal model. Dev Neurosci 2005 Aug;27:81-86.

Vannucci SJ, Hagberg H. Hypoxia-ischemia in the immature brain. J Exp Biol 2004 Aug;207(Pt 18):3149-54.

Vexler ZS, Ferriero DM. Molecular and biochemical mechanisms of perinatal brain injury. Semin Neonatol 2001 Apr;6(2):99-108.

Wagner CL, Eicher DJ, Katikaneni LD, Barbosa E, Holden KR. The use of hypothermia: a role in the treatment of neonatal asphyxia? Pediatr Neurol 1999 Jul;21(1):429-43.

Wang GJ, Deng HY, Maier CM, Sun GH, Yenari MA. Mild hypothermia reduces ICAM-1 expression, neutrophil infiltration and microglia/monocyte accumulation following experimental stroke. Neuroscience 2002;114(4):1081-90.

Wilkinson ID, Mitchel N, Breivik S, Greenwood P, Griffiths PD, Winter EM, Van Beek EJ. Effects of creatine supplementation on cerebral white matter in competitive sportsmen. Clin J Sport Med 2006 Jan;16(1):63-7.

Wyss M, Kaddurah-Daouk R. Creatine and creatinine metabolism. Physiol Rev 2000 Jul;80(3):1107-213.

Yager JY, Asselin J. The effect of pre hypoxic-ischemic (HI) hypo and hyperthermia on brain damage in the immature rat. Brain Res Dev Brain Res 1999 Nov;117(2):139-43.

Yager JY, Brucklacher RM, Vannucci RC. Cerebral energy metabolism during hypoxia-ischemia and early recovery in immature rats. Am J Physiol 1992 Mar;262(3 Pt 2):H672-H677.

Yenari MA, Han HS. Influence of hypothermia on post-ischemic inflammation: role of nuclear factor kappa B (NFkappaB). Neurochem Int 2006 Jul;49(2):164-9.

Zhao Y, Xu JX. The operation of the alternative electron-leak pathways mediated by cytochrome c in mitochondria. Biochem Biophys Res Commun 2004 May;317(4):980-7.

Zhu S, Li M, Figueroa BE, Liu A, Stavrovskaya IG, Pasinelli P, Beal MF, Brown RH, Jr., Kristal BS, Ferrante RJ, Friedlander RM. Prophylactic creatine administration mediates neuroprotection in cerebral ischemia in mice. J Neurosci 2004 Jun;24(26):5909-12.